The Holocene estuarine and coastal dune deposits of Soulac-sur-Mer (Médoc peninsula, southwest France)

Pascal Bertran, Pierrick Fouéré

Quaternaire, **31**, (3), *2020*, p. 231-248

THE HOLOCENE ESTUARINE AND COASTAL DUNE DEPOSITS OF SOULAC-SUR-MER (MÉDOC PENINSULA, SOUTHWEST FRANCE)

Pascal BERTRAN[1,2] & Pierrick FOUÉRÉ[1,3]

ABSTRACT

The rescue archaeological works carried out on the beach of Soulac-sur-Mer (Médoc, France) made it possible to clarify the stratigraphy, depositional context and chronology of the Holocene estuarine and aeolian formations currently eroded by the Atlantic Ocean. A first phase of deposition of homogeneous silty clay occurred in a mudflat context in a small tributary of the Gironde estuary, between about 7.1 ka and 4.9 ka cal BP. The later phases resulted in alternating clay sedimentation, peat and hydromorphic soil development showing desiccation cracks (upper intertidal context), erosion and tidal channel formation. The sequence was covered by peat with cattle footprints and herbaceous hummocks, presumably in a freshwater marsh context. Comparison of the ages obtained on this sequence with those from other marshes along the Gironde estuary shows a relatively similar evolution. The distribution of radiocarbon ages suggests that mud sedimentation was rapid between 6.5 and 5.5 ka cal BP in all the marshes, then gradually slowed down due to plugging and gradual reduction of the available sedimentation space. The alternation of sedimentation phases, peat development and soil formation is thought to reflect the fluctuations in flood frequency during the Holocene. The uppermost peat with footprints dates back to the Early Middle Ages. It was covered by aeolian deposits around 1.6 ka, which coincide with a climatic degradation (Dark Ages Cold Period) already identified elsewhere in the aeolian record of southwest France. A second generation of dune deposits, strongly disturbed by cattle trampling, then took place during the Little Ice Age.

Keywords: estuarine marshes, coastal dunefield, Médoc, France

RÉSUMÉ

LES DÉPOTS ESTUARIENS ET DUNAIRES HOLOCÈNES DE LA CÔTE ATLANTIQUE À SOULAC-SUR-MER (MÉDOC, FRANCE)

L'opération d'archéologie préventive menée sur la plage de Soulac-sur-Mer (Médoc, France) a permis de préciser la stratigraphie, le contexte de sédimentation et la chronologie des formations estuariennes et dunaires holocènes érodées par l'océan. Une première phase de dépôt de vases estuariennes homogènes se produit en contexte de slikke dans un vallon tributaire de la Gironde, entre environ 7,1 ka et 4,9 ka cal BP. Les phases ultérieures se traduisent par une alternance de phases de sédimentation argileuse, de phases de développement de tourbe ou d'un sol hydromorphe à fentes de dessiccation (contexte de schorre) et de phases d'érosion et de creusement de chenaux tidaux. La séquence se termine par un niveau de tourbe à empreintes de bétail et buttes d'herbacées, vraisemblablement en contexte de marais d'eau douce. La comparaison des âges obtenus sur cette séquence avec ceux provenant d'autres marais estuariens en bordure de la Gironde montre une évolution relativement similaire. La distribution des âges radiocarbones suggère que la sédimentation vaseuse a été très rapide entre 6,5 et 5,5 ka cal BP dans l'ensemble des marais, puis s'est progressivement ralentie en raison de leur colmatage et de la réduction de l'espace disponible. L'alternance de phases de sédimentation et de phases de tourbification ou de pédogenèse reflèterait des fluctuations de la fréquence des crues au cours de l'Holocène. La tourbe sommitale à empreintes date du Haut-Moyen Age. Elle a été recouverte par des dépôts dunaires vers 1,6 ka, qui coïncident avec une dégradation climatique (Dark Ages Cold Period) déjà identifiée ailleurs dans les Landes. Une seconde génération de dépôts dunaires, fortement perturbés par le piétinement du bétail, se met ensuite en place pendant le Petit Age Glaciaire.

Mots-clés : marais estuariens, massif dunaire côtier, Médoc, France

1 - INTRODUCTION

The Pleistocene and Holocene formations outcropping along the Atlantic coast at the tip of the Médoc peninsula have been the subject of many studies since the pioneering work of Fabre (1939), notably by Elhaï and Prenant (1963), Dubreuilh (1976), Tastet (1999), O'Brien and Jones (2003), Bosq *et al.* (2019) and Stéphan *et al.* (2019). At the same time, other authors have focused on the marshes bordering the Gironde estuary upstream, particularly Diot *et al.* (1999, 2002) and Clavé (2001). The extensive surveys made in these studies and ^{14}C dating have allowed determining the main stages of the evolution of the estuary during the Holocene. Aeolian formations also gave rise to recent studies thanks to the development of luminescence dating methods (Clarke *et al.*, 1999, 2002; Sitzia *et al.*, 2015; Bertran *et al.*, in press). As a result, the architecture of the Quaternary geological formations is known in broad lines, although the various studies are not always concordant. In particular, they reveal multiple generations of fluvial and estuarine deposits ranging from the Lower

[1] Inrap, 140 avenue du Maréchal Leclerc, FR-33130 BÈGLES. *Emails*: pascal.bertran@inrap.fr, pierrick.fouere@inrap.fr
[2] PACEA, UMR 5199, CNRS-Université de Bordeaux, bâtiment B2, allée Geoffroy-Saint-Hilaire, FR-33615 PESSAC.
[3] TRACES, UMR 5608, University Toulouse Jean Jaurès, Maison de la Recherche, 5, allée Antonio Machado, FR-31058 TOULOUSE cedex 9.

Manuscrit reçu le 28/04/2020, accepté le 20/08/2020

Pleistocene to the Holocene. Sandy aeolian deposits also show variable ages, ranging from the Middle and Late Pleistocene (Marine Isotopic Stages (MIS) 10 to 2) for the coversands ("Sable des Landes" Formation) to the historical period for the coastal dunefield.

Rescue archaeology work carried out during the dismantling of the riprap protecting the "Sables d'Argent" campsite at Soulac-sur-Mer from marine erosion made it possible to make new observations on the shoreline, both in plan view from the deposits exposed on the beach and in cross-section from trenches. The purpose of this article is to report on these observations, to propose a chronological framework based on new radiocarbon and optically stimulated luminescence (OSL) dating, and to place the evolution of the sedimentary context within the previously proposed paleoenvironmental framework.

2 - METHODS

As part of the archaeological work, trenches were excavated on the beach at low tide with an excavator and precisely located with a tacheometer. One or more sections per trench, between 2 and 3 m deep, were manually cleaned, described in detail and sampled for dating. The samples were sieved with water and wood and charcoal fragments were selected and sent to Beta Analytic (Miami) for AMS-^{14}C dating. Age calibration was made using Intcal13 curve and Calib 7.04 software. The dune deposits, which outcrop along the coastal cliff, were also surveyed and three samples were taken for OSL dating at the Luminescence Laboratory in Sheffield (UK). The OSL samples were collected by hammering a metal tube (60 mm in diameter, 250 mm long) into the freshly exposed section. The samples were sieved and chemically treated to extract 90 to 180 µm diametre quartz grains. The OSL measurements were undertaken on 9.6 mm single aliquot discs in a Risø automated luminescence reader. Equivalent dose (De) determination was carried out using the Single-Aliquot Regenerative-dose (SAR) and the age was extracted using the Central Age Model (CAM). Further details on the dating protocol are available in Bertran *et al.* (2020).

To compare the chronological data obtained with those already available in the literature for the Gironde marshes, the numerical ages were compiled and the distribution was analysed using the Kernel Density Estimation (KDE) and Cumulated Density Function (CPF) methods proposed by Vermeesch (2012). The KDE makes it possible to estimate the age distribution of sediments from the population of measured ages. As indicated by Vermeesch (2012), this method has many advantages over the commonly used cumulated age probability densities in that it avoids the false peaks created by the calibration of radiocarbon ages (Chiverell *et al.*, 2011) and the issues related to the variable uncertainty associated with radiocarbon ages. The processing was achieved using the densityplotter software (*http://densityplotter.london-geochron.com, last accessed 23.08.2020.*).

Because of marine erosion, the estuarine clays and peats outcrop widely on the beach. A detailed photogrammetric survey of the outcrops was made using a drone. This survey was complemented by satellite photographs available in Google Earth, in order to document the general distribution of the deposits. All the field data were georeferenced and processed in a geographic information system (GIS) using the QGIS software (version 3.4). To complete the data collected during this study and to place the site in a broader context, the boreholes stored in the Banque du Sous-Sol (BSS) of the Bureau des Recherches Géologiques et Minières (BRGM) were also consulted.

3 - GEOLOGICAL SETTING

The study area is located on the seashore south of Soulac-sur-Mer, at the northern tip of the Médoc Peninsula (fig. 1A). According to the 1:50,000 geological map (BRGM, *http://infoterre.brgm.fr/*), the Médoc is made up of a succession of alluvial terraces decreasing in altitude and becoming increasingly younger towards the north (fig. 1B). The terraces testify to the progressive incision of the river during the Pleistocene and the northward migration of the estuary. No numerical age is currently available for these fluvial sediments with the exception of the Fxb terrace, which has been the subject of preliminary ESR dating at Jaudignac and Loirac (altitude 5 m NGF; H. Tissoux, written communication). The age obtained places the gravel deposition at 850 ± 170 ka, i.e. in the Lower Pleistocene.

According to the borehole data stored at the BSS, the elevation of the substrate of Oligocene limestone decreases northward on average. At the study site, the gravels rest on the limestone at approximately -8 to -10 m NGF. However, the grid of available boreholes remains insufficiently dense in the area to get a precise image of the bedrock topography. Figure 1A shows significant local variations, whose distribution appears to be random. Allen *et al.* (1974), taking up Féral (1970), proposed that the depressions correspond to Holocene palaeochannels of the Gironde estuary, one of the branches running through the Lède du Gurp ("Chenal du Gurp"), the other further north through the study area ("Chenal de Soulac"). At the Lède du Gurp, this interpretation relied on the presence of Holocene peat outcropping on the coast, which has provided evidence of pre- and protohistoric occupation. Following recent coastal erosion, the peats were found to fill an approximately circular depression of presumably karstic origin (doline) instead of an old channel (Faye *et al.*, 2019). Intense karstification of the Oligocene limestones had previously been highlighted by Courrèges (1997) from the study of the shelf off the Pointe de la Négade (fig. 1A). Karstification is believed to be also at the origin of the large depressions visible on the emerged part of the Médoc peninsula, such as the Reysson marsh south of the study area, which is interpreted as a polje. The local depression traversed by the borehole BSS001UZCX (fig. 1B) is interpreted here in the same way.

At the tip of the peninsula, the Pleistocene fluvial gravels are covered by transgressive Holocene estuarine deposits noted Fyb and MFyb on the geological map (Dubreuilh and Marionnaud, 1972), themselves covered by the coastal dunefield (Dz). In the study area, Pontee *et*

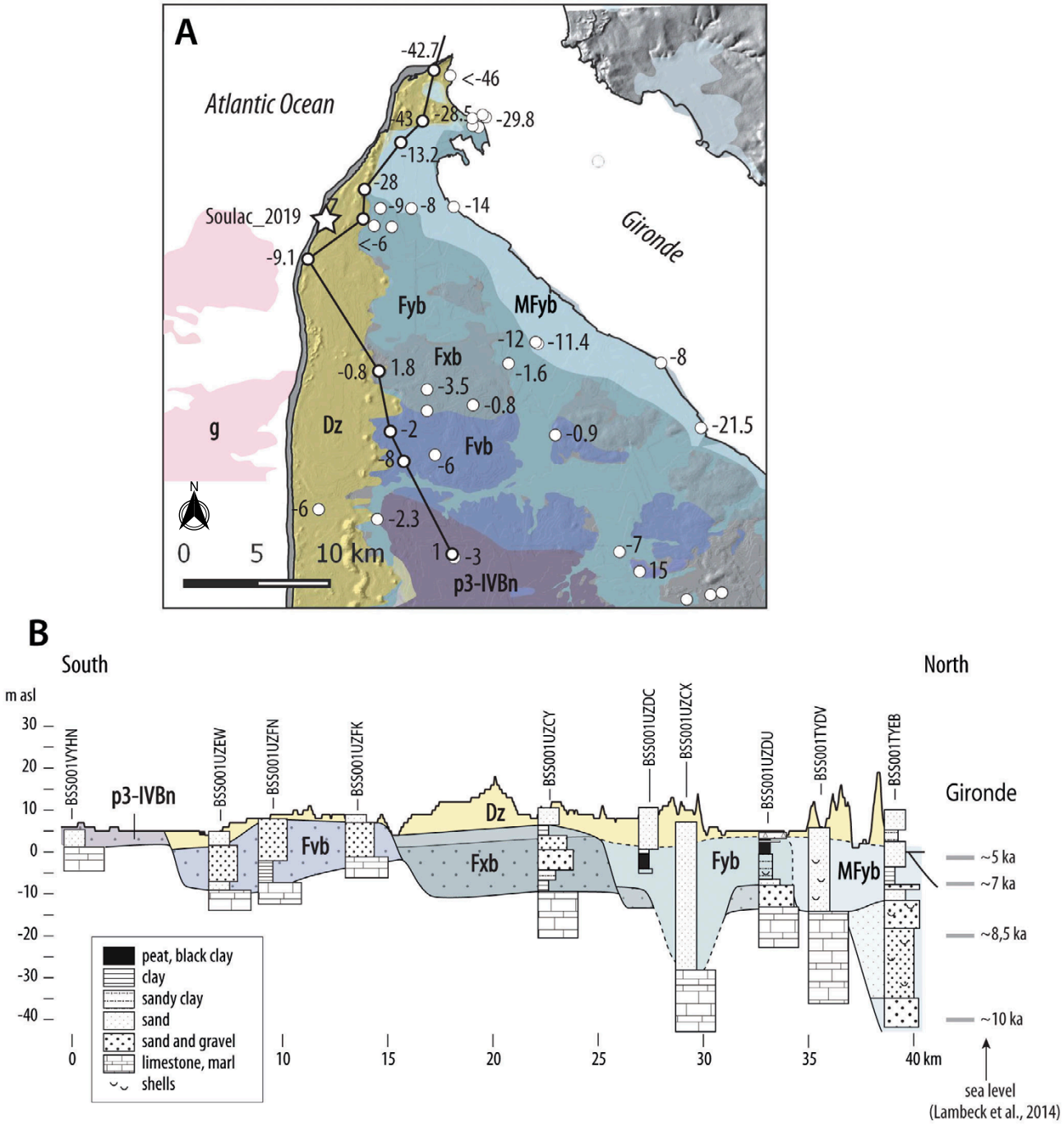

Fig. 1: A - Geology of the study area (from the harmonized geological map at 1:50,000, *http://infoterre.brgm.fr/*), and location of the survey site; the numbers correspond to the elevation of the limestone substrate (in m NGF); B - Schematic north-south section of the Médoc peninsula according to the boreholes stored at the Banque du Sous-Sol (Bureau des Recherches Géologiques et Minières).

Fig. 1 : A - Extrait de la carte géologique harmonisée à 1/50 000 (http://infoterre.brgm.fr/) et localisation du site étudié ; les chiffres correspondent à l'altitude du substratum calcaire (en m NGF) ; B - Coupe schématique nord-sud de la péninsule du Médoc d'après les sondages de la Banque du Sous-Sol du BRGM.

al. (1998) suggested that the clays and peats outcropping on the Atlantic coast corresponded to deposits filling a former tributary of the Gironde estuary, which is currently cut by the shoreline. The cross-sectional profile of the peninsula from the available boreholes at the BSS (fig. 2) is consistent with this interpretation and shows that (i) the base of the clays and peats has a decreasing elevation towards the Gironde estuary, (ii) their thickness increases in the same direction, and (iii) the grain size becomes coarser towards the estuary, suggesting river-fed sedimentation. Accordingly, the fine-grained units do not correspond to a former channel open to the ocean, but to one of the many marshes on the margin of the estuary resulting from the Holocene transgression and later brought to outcrop on the Atlantic coast because of the gradual retreat of the coast.

Current estuarine sedimentation has been described in detail by Allen *et al.* (1974) and Virolle *et al.* (2019). The lithofacies typically include (i) interbedded sands and clays in the subtidal zone (central area of the estuary) linked to tide-controlled fluctuations in current strength, (ii) sands with varying amounts of clay in the tidal bars, (iii) bedded or massive silts and clays in the intertidal zone (mudflat) and (iv) organic clays with plant debris in the upper intertidal/supratidal zone colonised by vegetation (salt marsh).

These areas are clearly identifiable in aerial photographs along the estuary (fig. 3). Mudflats and salt marshes

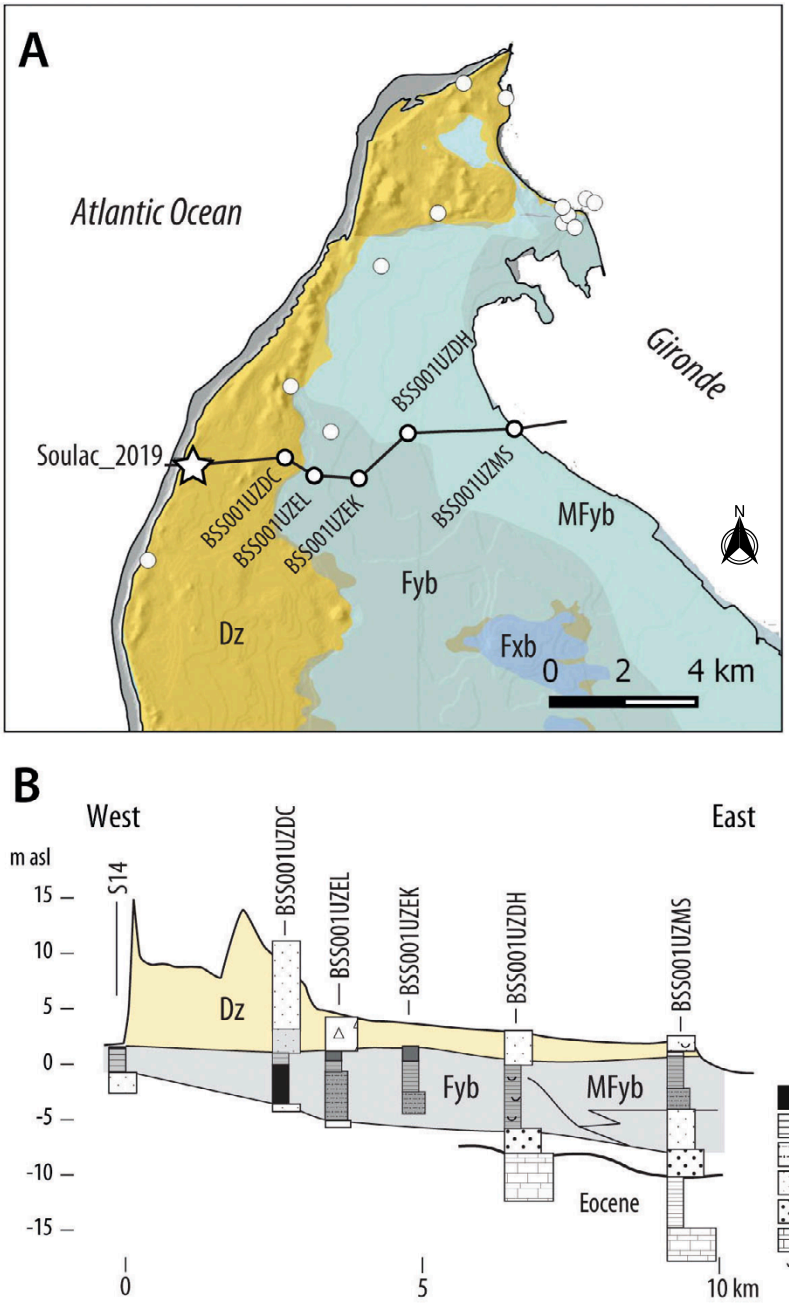

Fig. 2: A - Geology of the study area and location of the west-east section; B - Schematic west-east section of the Médoc peninsula according to the boreholes stored at the Banque du Sous-Sol. S14: trench 14 (this study).

Fig. 2 : A - Extrait de la carte géologique harmonisée à 1/50 000 (infoterre.brgm.fr) ; B - Coupe schématique ouest-est de la péninsule du Médoc d'après les sondages de la Banque du Sous-Sol du BRGM. S14: tranchée 14 (cette étude).

fringe areas of marshes that are only exceptionally covered by floods and are widely cultivated ("mattes": marshes reclaimed from the XVIIIth century and bounded by a dyke, noted MFyb on the geological map; "palus": marshes that were fixed earlier, noted Fyb). Multiple tidal channels that form a dendritic network, often with a bayonet-shaped layout, cross the mudflats and salt marshes. Channel bottom sediments are clayey sand with clay pebbles and shell debris, while the banks are covered with clayey silt showing desiccation cracks (fig. 3E). These drapes can have a steep slope (15-20°).

4 - RESULTS

4.1 - DESCRIPTION OF THE HOLOCENE OUTCROPS ERODED BY THE OCEAN

Rapid erosion of the coast periodically uncovers Holocene clays and peats on the beach between Amélie and Soulac-sur-Mer. These deposits are visible on satellite photographs accessible from Google Earth, particularly the 2017 cover that served as the basis for the map proposed in Figure 4. The deposits have already been the subject of detailed studies by Clavé (2001) and Stéphan *et al.* (2019). Following the retreat of the coast, the outcrops visible in 2017 largely disappeared and new areas were exhumed at the time of archaeological investigation.

Figure 5 shows the outcrop pattern as of April 2019. It schematically shows the following units:

(1) Greenish silty clay outcropping broadly at the lower foreshore [US 1019]. It is capped by a thin layer of black peaty clay [US 1016]. Stratification is subhorizontal when identifiable. The clays are affected by a polygonal network of desiccation cracks (fig. 6A, E).

(2) Discontinuous sandy gravel, locally rich in pebbles of ferruginous sandstone [US 1015], eroding the green clay (fig. 7A, C). The pebbles are concentrated in furrows (fig. 7E).

(3) Grey clay arranged in layers with a gentle dip (2-5°)

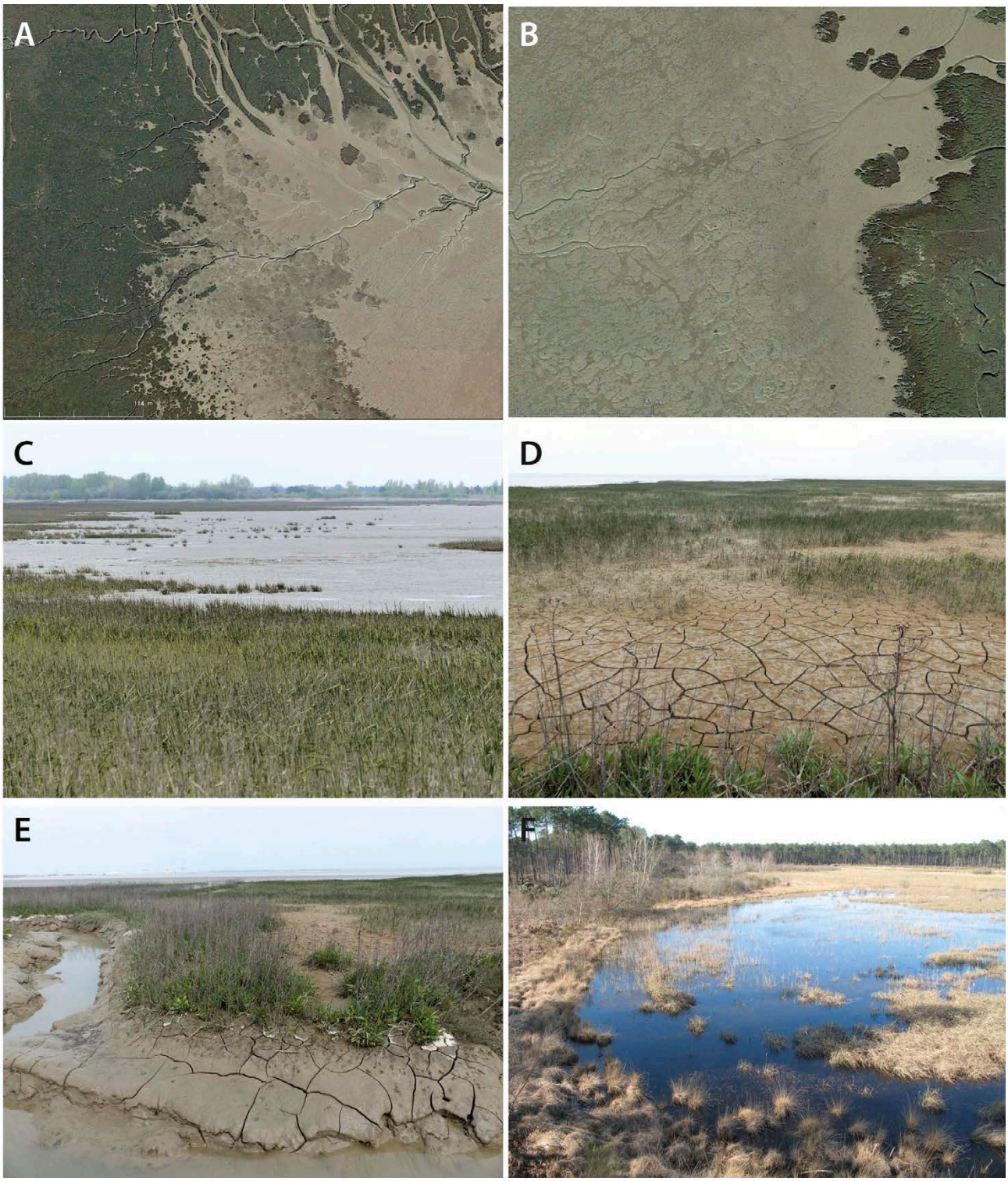

Fig. 3: A, B - Aerial view of the mudflat and salt marsh with halophilic plants in the current Gironde estuary (Google Earth); dendritic tidal channels can be seen; C - View of the mudflat-salt marsh transition at Soulac-sur-Mer; D - Area with large desiccation cracks in the salt marsh zone; E - Channel covered with mud showing desiccation cracks; note the steep slope of the banks; F - Freshwater marsh near Hostens (south of Bordeaux) with tussocks of *Poacea*.

Fig. 3 : A, B - Vue aérienne de la slikke et du schorre à couvert végétal halophile le long de l'estuaire actuel de la Gironde (Google Earth) ; on distingue les nombreux chenaux de marée dendritiques ; C - Vue de la transition schorre-slikke à Soulac-sur-Mer ; D - *Zone à grandes fentes de dessiccation dans la zone de schorre ; E - Chenal tapissé de vase à fentes de dessiccation ; noter la pente élevée des berges ; F - Marais d'eau douce près d'Hostens (sud de Bordeaux) à touffes de molinie.*

towards the east [US 1014]. To the north of the study area (fig. 4), the clays are arranged in steeply dipping beds that form NNW-SSE oriented ridges emerging from the current beach sands. These layers correspond to bank deposits in tidal channels that cut through the first generation of estuarine deposits.

(4) Organic clays overlain by a thin layer of hummocky peat with cattle footprints [US 1002] (fig. 8A, B, C). The peat is roughly horizontal and shows the juxtaposition of areas intensely trampled by cattle and areas with small hummocks (~10-20 cm high) whose top is covered by herbaceous remains (fig. 8B) or, sometimes, by a shrub stump. In the area under the former riprap, the peat topography is more irregular. The peat drapes grey clay reliefs (30 to 50 cm high) and small channels (~1 to 2 m wide; 20-50 cm deep) rich in cattle footprints (fig. 8E, F).

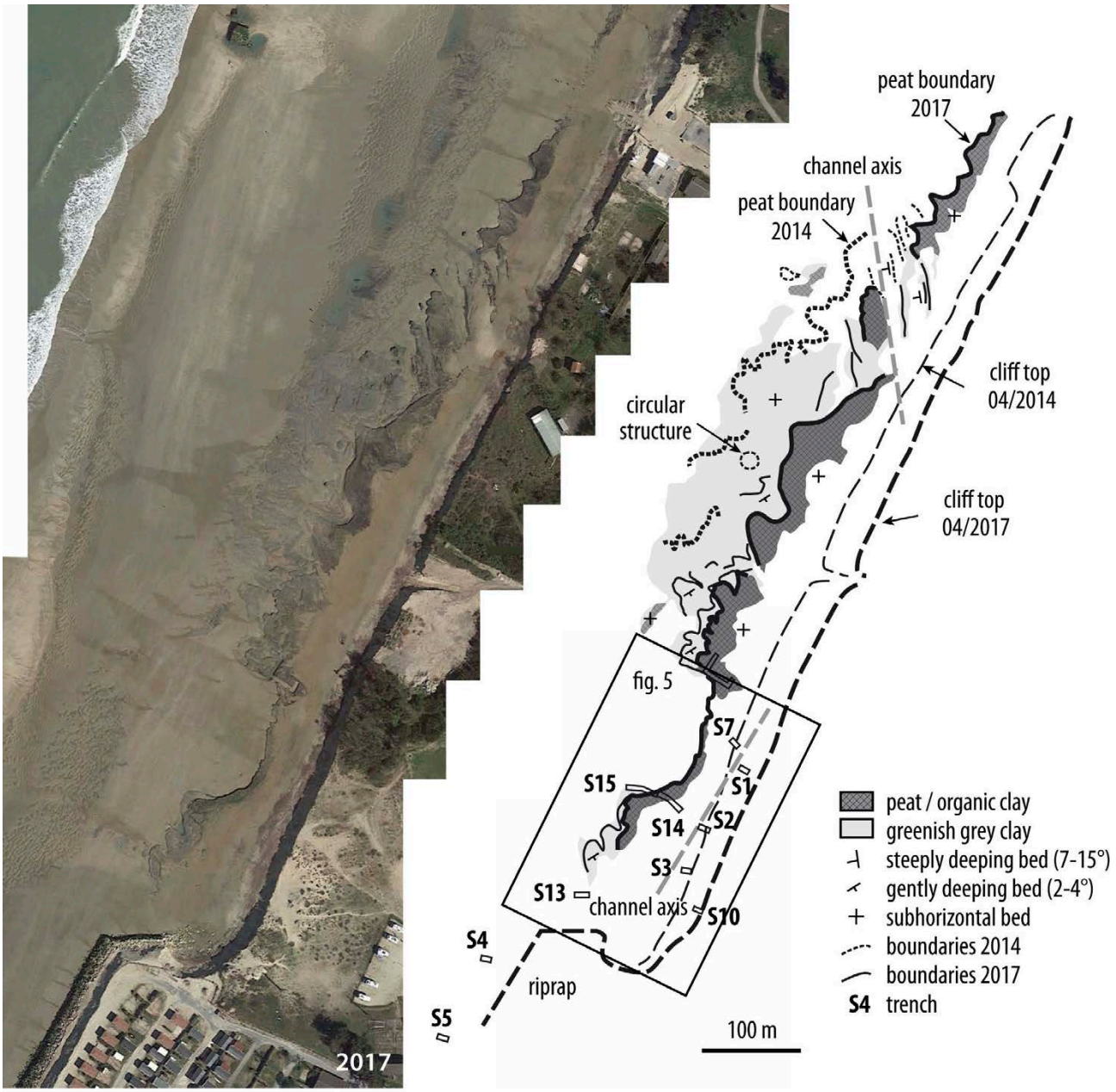

Fig. 4: Aerial photograph of the study area (Google Earth, 2017) and interpretation.
The location of the 2019 trenches is indicated.
Fig. : Photographie aérienne de la zone étudiée (Google Earth, 2017) et interprétation. La localisation des sondages est indiquée.

4.2 - STRATIGRAPHY OF THE ESTUARINE DEPOSITS

The main units observed in trenches are the following, from the oldest to the most recent (fig. 9):

(1) Clean, cross-bedded grey sand, sometimes with small gravel (0.5-1 cm diametre), overlain by horizontally bedded sand (US 1022). This level, which forms the base of the sequence, was observed over a thickness of about 1 m in trenches S4 and S5. It is tentatively interpreted here as classical fluvial bar deposits (in a non-estuarine context) because of the poor clay content and the lack of shell fragments. The bedded sand is covered by massive, slightly clayey, oxidized sand with bioturbation and abundant roots (fig. 10A, B), which corresponds to a hydromorphic palaeosol and reflects an interruption of sedimentation.

(2) Greenish grey clayey sand with some gravel, green clay pebbles and wood fragments, 40 to 60 cm thick (US 1021). This unit is interpreted as flood deposits. The presence of clay pebbles originating from the reworking of mudflat deposits indicates that the site was at that time already located in an estuarine context.

(3) Homogeneous greenish grey (10GY 4/1) to dark greenish grey (5GY 3/1) plastic silty clay up to 1.4 m thick (US 1019). The clays usually show smooth and striated surfaces (slickensides) due to alternating shrinkage and swelling (fig. 7B) and contain abundant oxidation spots in the upper part. In trench S12, a level rich in *Scrobicularia* shells was observed at about -1.2 m NGF. These clays correspond to mudflat deposits. In a trench (S12), a discontinuity is visible within the clays and indicates a relatively long desiccation phase. It is marked by a polygonal network of desiccation cracks (fig. 7A, C); the

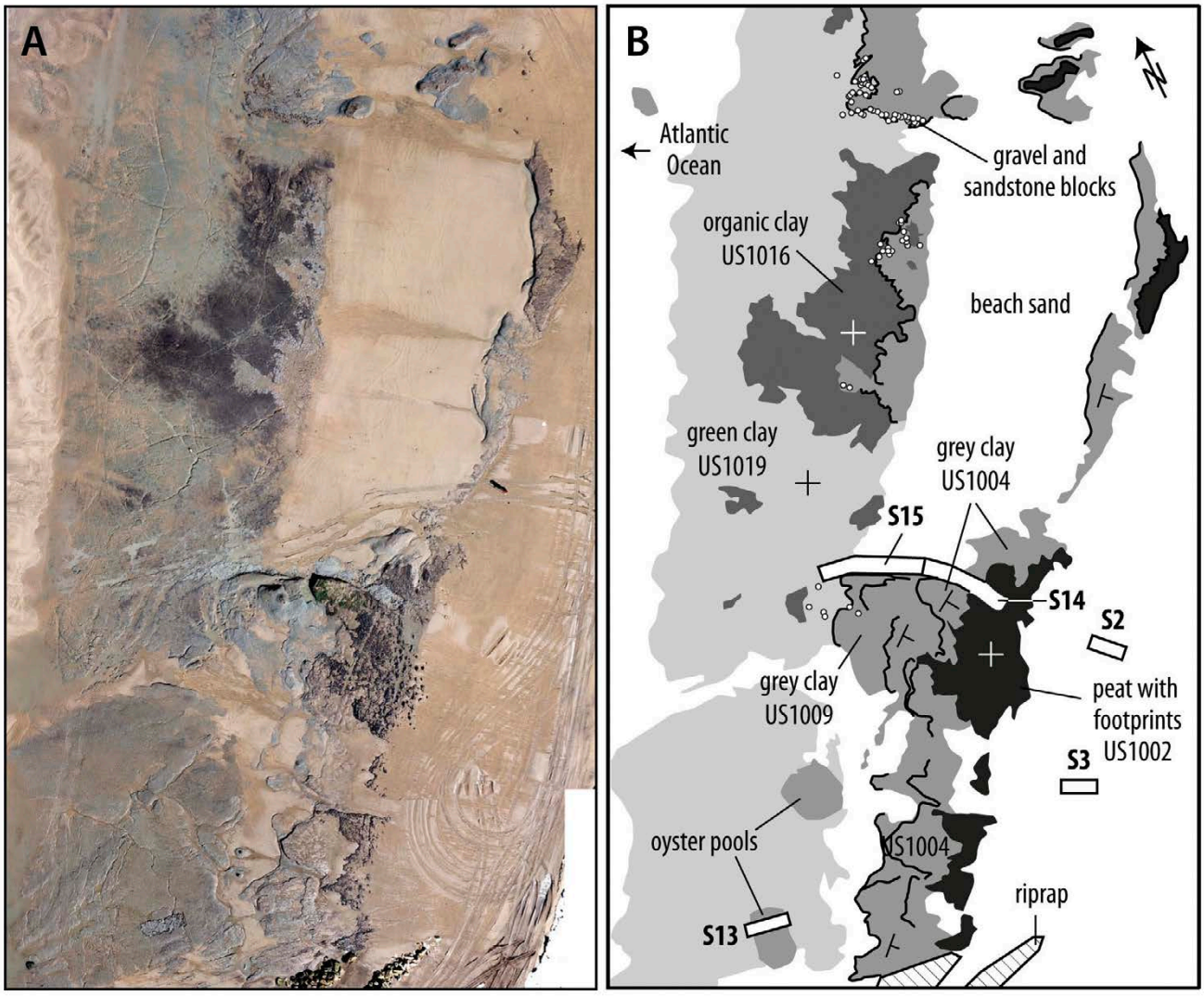

Fig. 5: Photograph of the outcrops (W. O'Yl, Inrap) uncovered by the ocean in 2019 (A) and interpretation (B).
The location of the photographed area is shown in Figure 4.
Fig. 5 : Photographie des affleurements (W. O'Yl, Inrap) découverts par l'océan en 2019 (A) et interprétation (B). L'emplacement de la zone photographiée est indiqué sur la Figure 4.

cracks 20 to 50 cm high are covered by bright green Fe precipitations, probably fougerite ("green rust") (Trolard, 2006). This suggests the initial formation of iron oxides followed by a secondary evolution in a reducing context linked to the resumption of clay sedimentation.

(4) Dark grey organic clay with abundant roots (2-10 cm thick) covered in some trenches by a thin layer of black peat (US 1016) (fig. 10A). This unit indicates a salt marsh-like environment and a near cessation of detrital inputs.

(5) Sand and gravel, locally rich in pebbles of clay and ferruginous sandstone [US 1015], whose base erodes the earlier units (fig. 10B). This unit is discontinuous; in trench S15, it plunges towards the east and forms the basal deposits of a palaeochannel up to 1 m deep (fig. 11). It thus attests to a phase of local erosion of the mudflat by a tidal channel. Archaeological remains (pottery shards, lithics and faunal remains) attributed to the beginning of the Early iron Age rest on these sands. They are mostly associated with salt production (briquetting).

(6) Homogeneous dark gray to dark greenish gray clay (10Y 4/1 to 5GY 4/1) cover the sand and fill the paleochannel (US 1009). They indicate a mudflat environment comparable to that of US 1019. These clays are oxidized in the upper decimetres and contain abundant small roots.

(7) In trench S14, a 5 to 10 cm thick dark grey clayey-sandy organic level (US 1011), rich in archaeological remains attributed to the Gallo-Roman period (Late Republican period, i.e. end of 1st century BCE / beginning of 1st century CE), covers the bioturbated grey clay. The sand fraction likely indicates aeolian inputs.

(8) Laterally, a tidal channel 1 to 1.5 m deep crosses the previous units. The stratigraphic relationship between the channel and the Gallo-Roman occupation level could not be specified in trench S14, as the contact zone was disturbed by later anthropogenic structures (oyster pool). The channel filling observed in trenches S1, 2, 3 and 14 comprises at the base dark grey sand with oyster and *Scrobicularia* shells and clay pebbles (US 1014), then well graded sand with current ripples (US 1013), black clay (5Y 2.5/1) with small desiccation cracks (US 1010) (fig. 7F) and homogeneous grey clay (2.5Y 4/1) (US 1004). This sequence reflects a phase of incision, followed by lateral migration and progressive plugging of the channel, probably in an upper intertidal environment rich in organic matter.

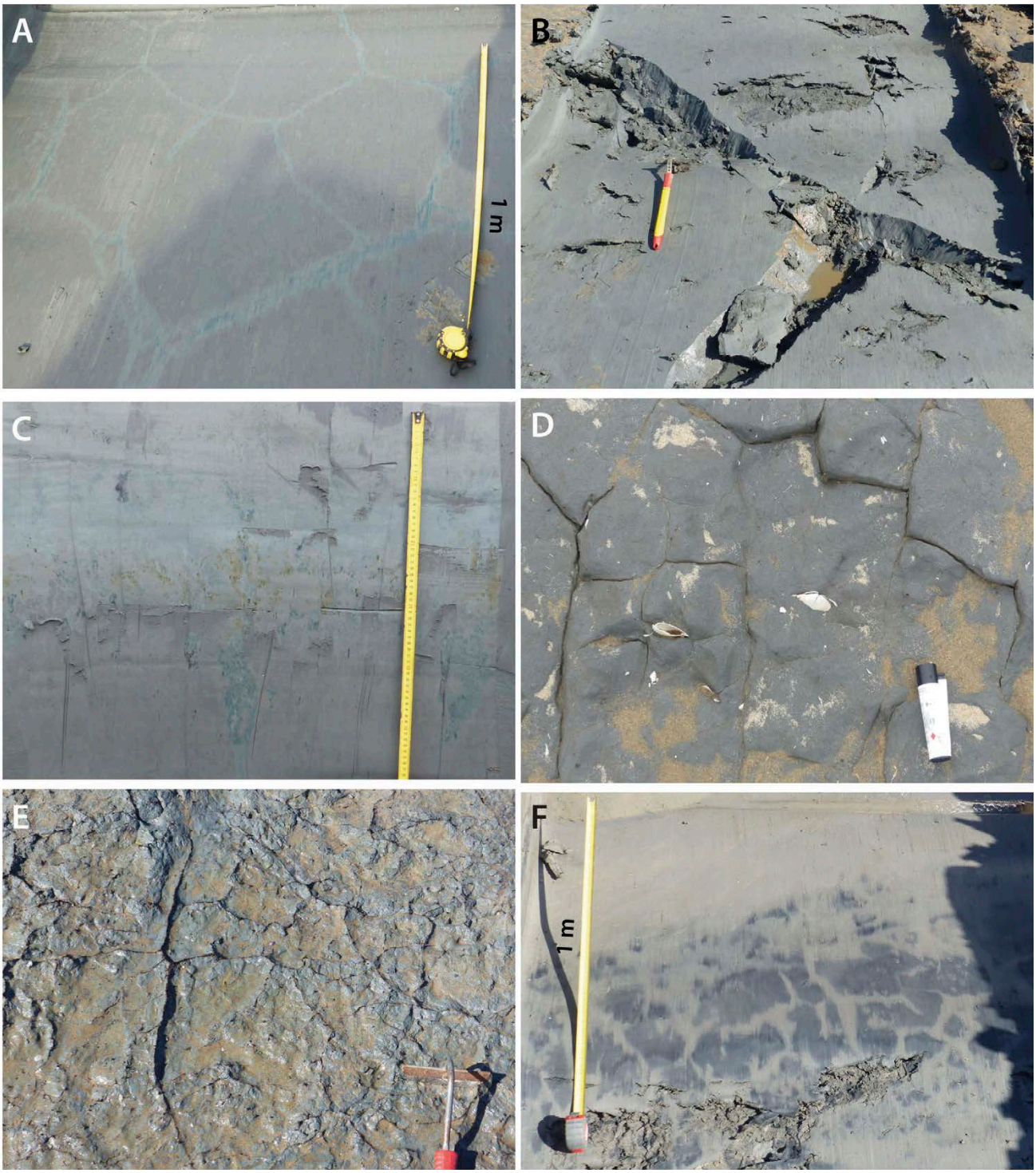

Fig. 6: Views of the clay facies.
A - Green clays with desiccation cracks, trench S5; B - Green clays with slickensides, trench S8; C - Desiccation cracks in greenish-grey clays and oxidation spots, trench S12; note the green filling of the cracks; D - Greenish-grey clays with *Scrobicularia* shells; E - Green clay with a polygonal desiccation network, oxidized at the surface; F - Black clay with a network of desiccation cracks, trench S2.
Fig. 6 : Vues des faciès argileux. A - Argiles vertes à fentes de dessiccation, sondage S5 ; B - Argiles vertes à slickensides, sondage S8 ; C - Niveau de fentes de dessiccation dans des argiles gris-vert et taches d'oxydation, sondage S 12 ; noter le remplissage vert des fentes ; D - Argiles gris vert à scrobiculaires ; E - Argile verte à réseau polygonal de dessiccation, oxydé en surface ; F - Argile noire à réseau de fentes de dessiccation, sondage S 2.

(9) The whole sequence is covered by root-rich black clay and a thin peat level with cattle footprints (US 1002). The hummocks capped by herbaceous remains are reminiscent of *Poacea* tussocks typical of regional freshwater marshes (fig. 8B).

(10) Grey dune sand burying the peat.

Overall, the sequence shows above fluvial sands, a succession of mudflat deposits separated by phases of reduced sedimentation, oxidation and vegetation development (salt marsh environment) or by phases of tidal channel incision and filling. These channels resulted from spontaneous incision and evolution of the marsh due to tidal currents (e.g., D'Alpoas *et al.*, 2007), possibly accelerated during major floods. The Gallo-Roman occupation occurred during one of the phases of vegetation development, while the Early Iron Age occupation took place near a newly created deep tidal channel.

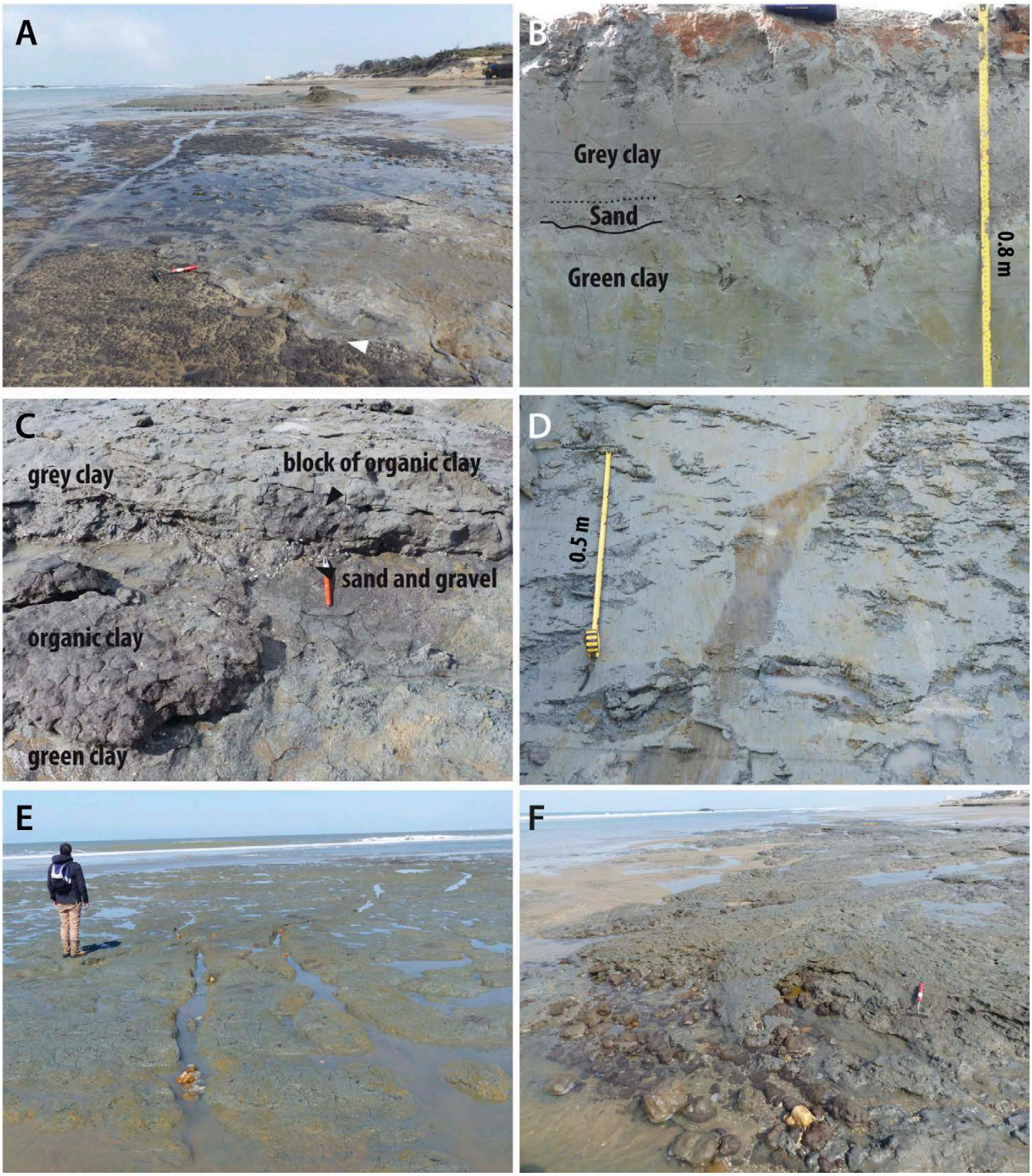

Fig. 7: Views of the coarse-grained facies.
A - Grey clays (US 1007-1009) overlying peaty clays (US 1016); the contact is indicated by the white arrow; B - Section showing a sandy level (US 1015) eroding the green clays (US 1019), trench S15; C - View of the contact between green clays (US 1019) and grey clays (US 1007-1009) underlined by sand (US 1015); black clay pebbles (US 1016) are visible at the base of the grey clays; D - Furrow filled with sand and gravel (US 1015) eroding the green clays, trench S15; E - idem, exhumed by current marine erosion; F - Fragments of ferruginous sandstone embedded in sand (US 1015).
Fig. 7 : Vue des faciès grossiers. A - Argiles grises (US 1007-1009) recouvrant des argiles tourbeuses (US 1016) ; le contact est indiqué par la flèche blanche ; B - Coupe montrant le niveau de sable (US 1015) érodant les argiles vertes (US 1019), sondage S15 ; C - Vue du contact entre l'argile verte (US 1019) et les argiles grises (US 1007-1009) souligné par un niveau de sable (US 1015) ; des galets d'argile noire (US 1016) sont visibles à la base des argiles grises ; D - Sillon rempli de sable et de gravier (US 1015) érodant les argiles vertes, sondage S15 ; E - idem, exhumé par l'érosion marine actuelle ; F - Fragments d'alios repris dans les sables (US 1015).

4.3 - CHRONOLOGICAL DATA OF THE ESTUARINE DEPOSITS

In the study area, radiocarbon dating has been already carried out during previous works (Stéphan *et al.*, 2019) (fig. 12). The age obtained on the sand immediately underlying the first clay layers (unit 2b of Stéphan *et al.*, 2019, equivalent to US 1021) is 6360 ± 30 BP, i.e. 7416-7183 cal BP (2σ). A wood fragment from the peaty clay (unit 3b from Stéphan *et al.*, 2019 equivalent to US 1016) that terminates the first generation of clayey deposits yielded an age of 6025 ± 50 BP, i.e. 6996-6742 cal BP (Early Neolithic). Wooden structures in the peaty clay gave an age of 3984 ± 70 BP, i.e. 4802-4236 cal BP (Late

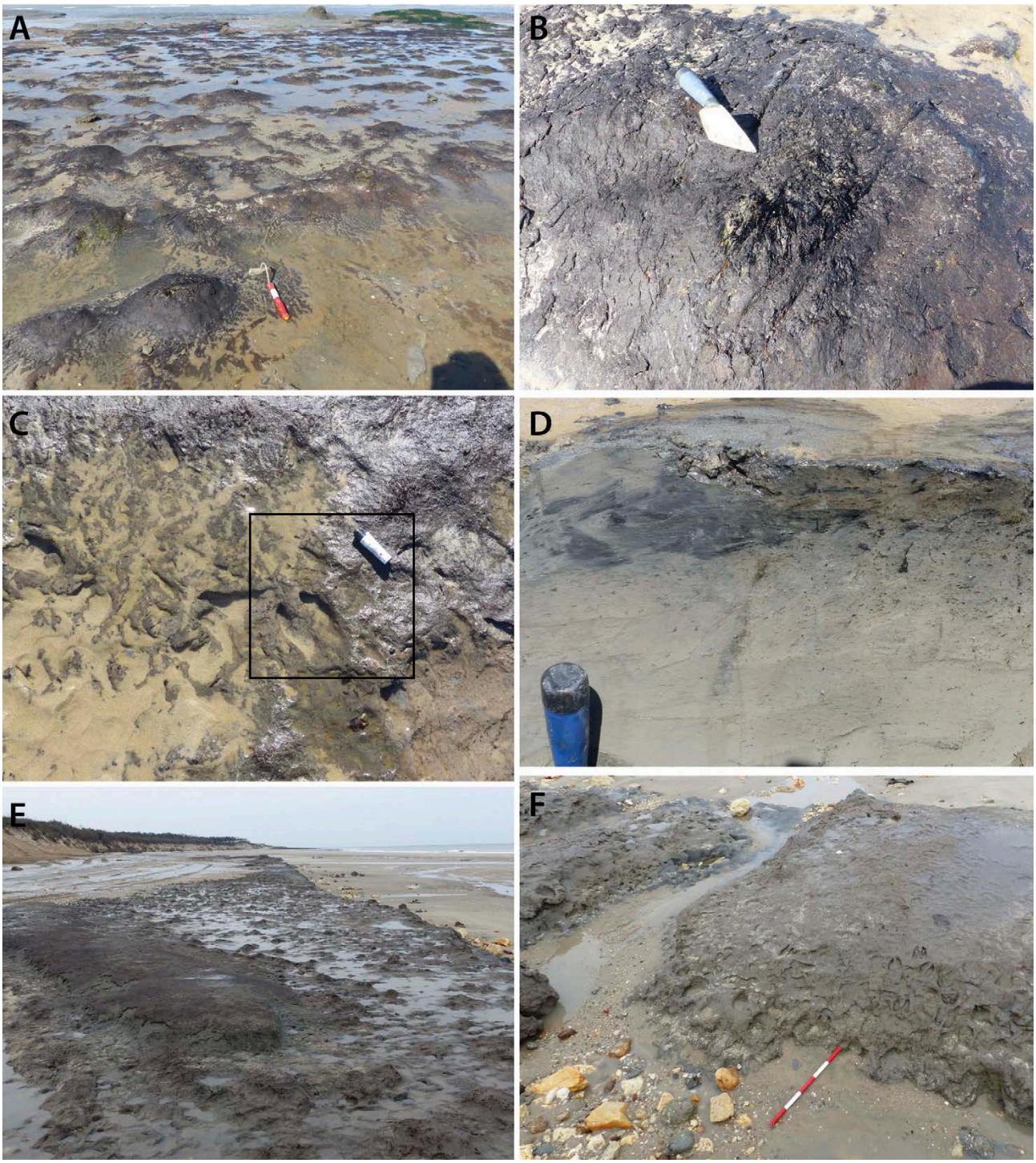

Fig. 8: Views of the peaty facies.

A - View of hummocky peat with footprints (US 1002); B - Detail of a hummock with remnants of herbaceous vegetation; C - Cattle footprints; D - Section view of the thin peat layer and dark grey clay, trench S3 ; the underlying light grey clays (US 1004) are perforated by abundant roots; E - Peat with footprints covering a small relief and a depression, area under the riprap; F - Small meandering channel with footprints along the banks, area under the riprap.

Fig. 8: Vues des faciès tourbeux. A - Vue de la tourbe à buttes et empreintes (US 1002) ; B - Détail d'une butte avec restes de végétation herbacée ; C - Empreintes de bétail ; D - Vue en coupe de la mince couche de tourbe et des argiles gris foncé, sondage S3 ; les argiles gris clair sous-jacentes (US 1004) sont perforées par de nombreuses racines ; E - Tourbe à empreintes nappant un petit relief et une dépression, zone située sous l'enrochement ; F - Petit chenal à méandres dont les berges sont parsemées d'empreintes, zone située sous l'enrochement.

Neolithic). Unit 4 (grey clays) of Stéphan *et al.* 2019 includes our US 1009 to 1004. Wooden posts driven into this unit provided an age of 2570 ± 40 BP, i.e. 2762-2495 cal BP (Early Iron Age). Oyster shells (possibly filling a structure identical to that (US 1003) identified in trench S14) gave an age of 2108 ± 74 BP, i.e. 1897-1510 cal BP (Gallo-Roman period). Lastly, wood from the upper peat (unit 5 of Stéphan *et al.*, 2019 equivalent to US 1002) gave an age of 1260 ± 60 BP, i.e. 1286-1070 cal BP (Early Middle Ages).

Six new radiocarbon ages were obtained during the archaeological work (fig. 9, Table 1). Root fragments taken from the top of the basal sand (US 1022) at about -1.8 m NGF gave an age of 6170 ± 30 BP, i.e. 7165 - 6980

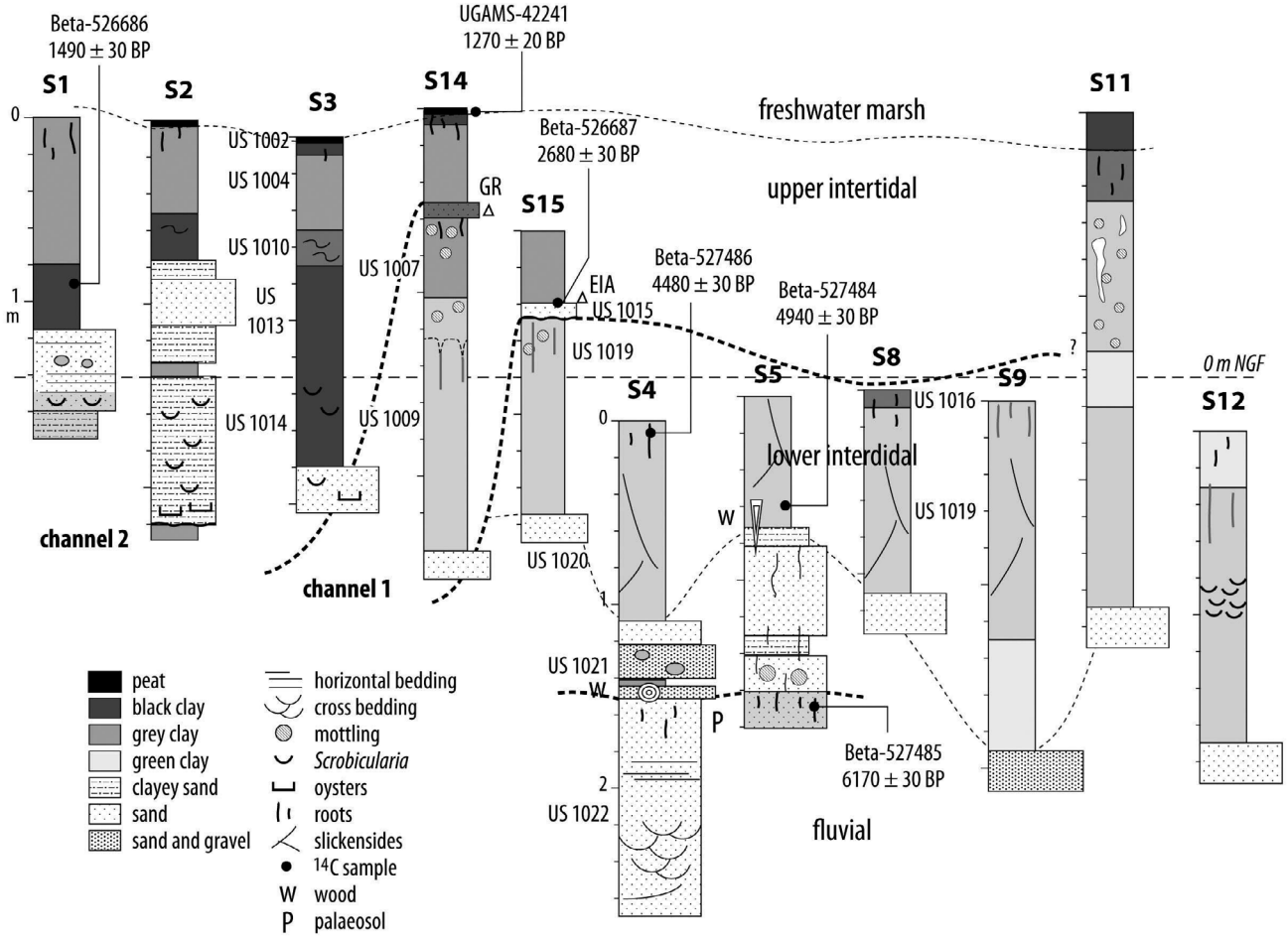

Fig. 9: Schematic stratigraphy of the trenches and location of dated samples.
Fig. 9 : Stratigraphie schématique des différentes tranchées et localisation des échantillons datés.

ref date	sample ref.	X WGS84	Y WGS84	Z (m asl)	method	material	age (a)	uncertainty	age (a) cal BP	age (a) cal BCE/CE	references
Beta-527485	T5-G13	1.1411	45,50	-1.8	14C	wood	6170	30	7165/6980	-5216/-5031	this study
Beta-527484	T5-G12	-1.1411	45,50	-0.7	14C	wood	4940	30	5726/5602	-3377/-3653	this study
Beta-527486	T4-G10	-1.1408	45,50	-0.3	14C	wood	4480	30	5290/4979	-3341/-3030	this study
Beta-526687	PRL-10	-1.14	45,50	+0.4	14C	wood	2680	30	2846/2751	-897/-802	this study
Beta-526686	PRL-07	-1.1392	45,50	+0.5	14C	charcoal	1490	30	1416/1504	436/644	this study
UGAMS-42241	PRL-04	-1.1391	45,50	+1.45	14C	wood	1270	20	1180/1270	680/770	this study

Table 1: Radiocarbon ages obtained from the estuarine deposits. Calibrated ages are given at 2 σ.
Tableau 1: Ages radiocarbone obtenus sur les dépôts estuariens. Les âges calibrés sont donnés à 2σ.

cal BP (Beta-527485). This age provides a maximum for the onset of the sedimentation in an estuarine context (clayey sand, US 1021), which is similar to that proposed by Stéphan *et al.* (2019).

A wood fragment from the lower part of the first generation of estuarine clays (US 1019) at about -0.7 m NGF yielded an age of 4940 ± 30 BP, i.e. 5726 - 5602 cal BP (Beta-527484). Root debris from the top of the same unit was dated at 4480 ± 30 BP, i.e. 5290 - 4979 cal BP (Beta-527486). These roots are related to the development of the peat (US 1016). The age of the peat is therefore substantially younger than that (6025 ± 50 BP) obtained on a wood fragment by Stéphan *et al.* (2019). The assumption that the latter fragment was reworked and that the age is not representative of the peat is favoured here.

A piece of wood found at the top of the US 1015 sands, presumably associated with the Early Iron Age occupation, yielded an age of 2680 ± 30 BP, i.e. 2846 - 2741 cal BP (Beta-526687), in accordance with the age expected from the archaeological data. Charcoal fragments collected in the most recent channel infill (US 1010) were dated to 1490 ± 30 BP, i.e. 1504 - 1306 cal BP (Beta-526686) (Early Middle Ages). Lastly, a wood fragment from the upper peat with footprints (US 1002) gave an age of 1270 ± 20 BP, i.e. 1180-1270 cal BP (UGAMS 42241), in agreement with the age obtained by Stéphan *et al.* (2019).

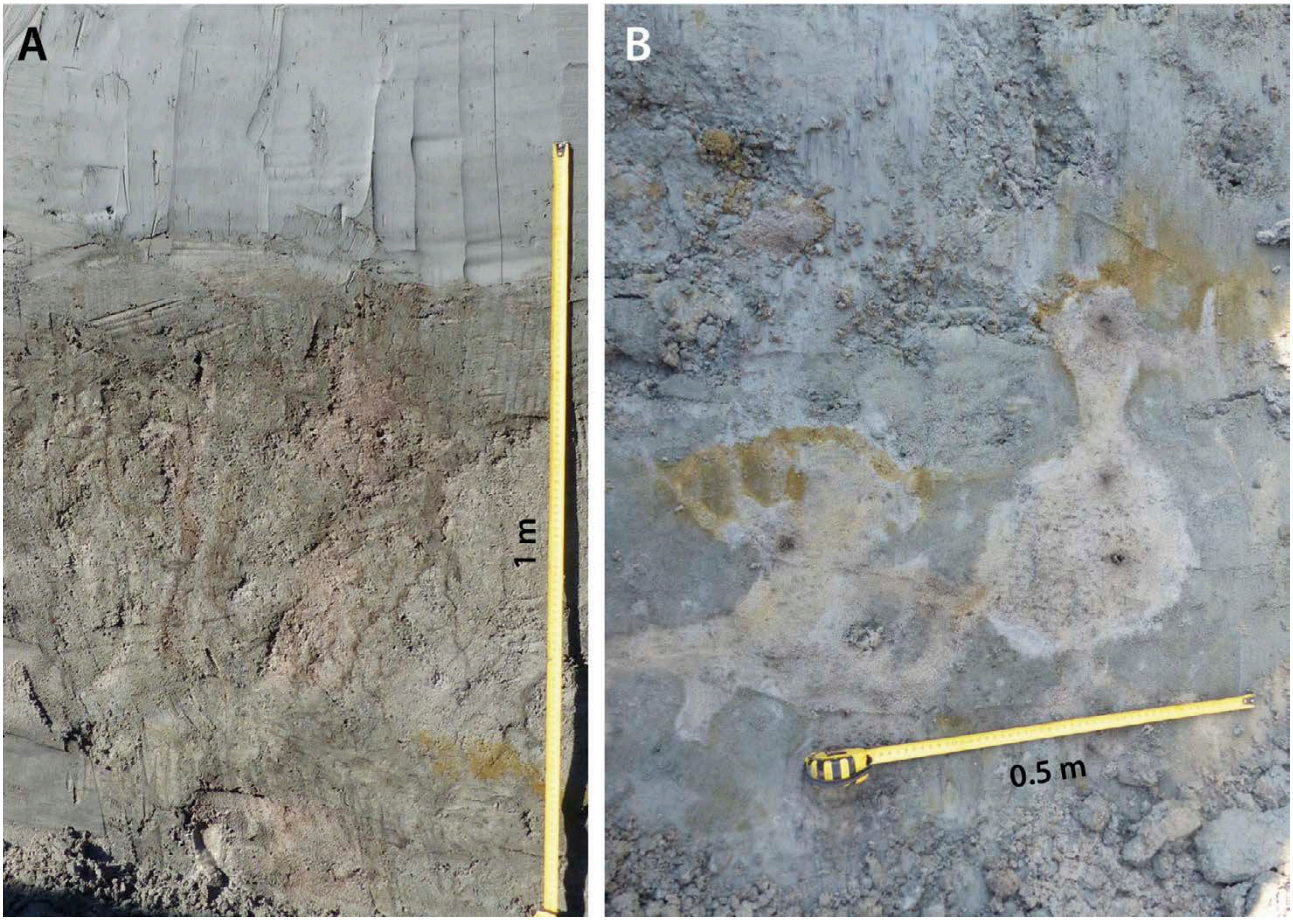

Fig. 10: Views of the palaeosol beneath the tidal clay units.
A - Bioturbed clayey sands (US 1021) beneath green clays, trench S5; B - Plan view through the palaeosol at the top of the US 1022 sands. Discoloured areas bordered by greenish-yellow ferruginous precipitation encircle the roots.
Fig. 10 : Vue du paléosol sous les dépôts argileux tidaux. A - Sables argileux bioturbés (US 1021) sous les argiles vertes, sondage S5 ; B - Vue en plan du paléosol au sommet des sables de l'US 1022. Les zones décolorées bordées de précipitations ferrugineuses jaune verdâtre entourent des racines.

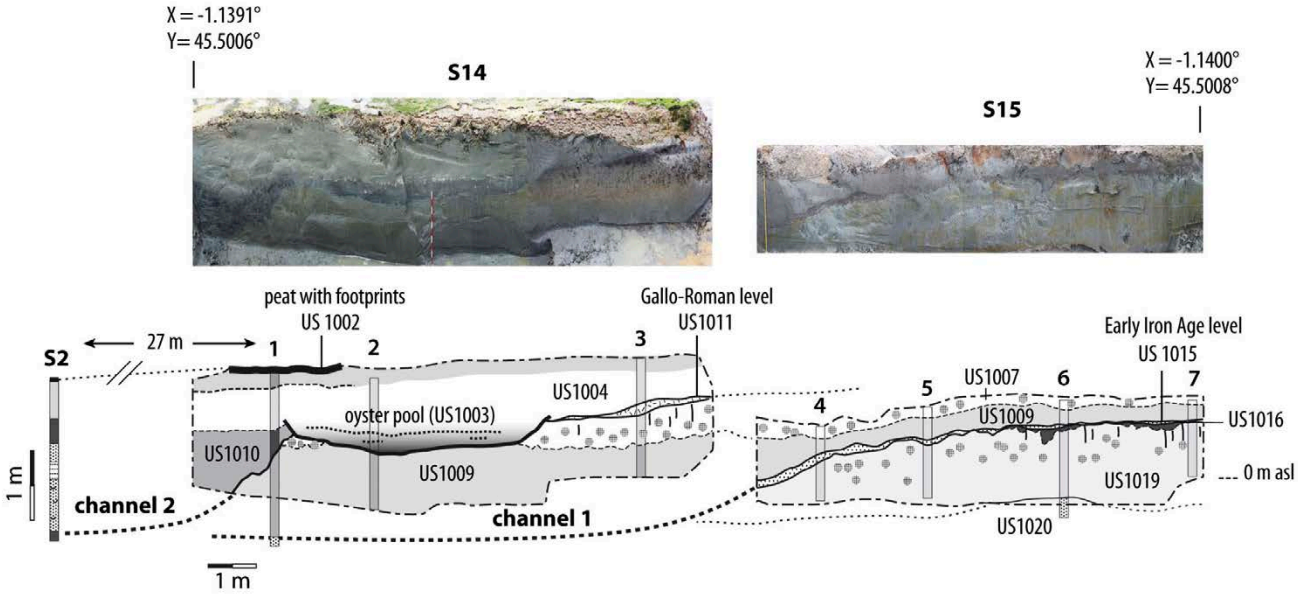

Fig. 11: Photograph of the south wall of trenches S14 and S15 and interpretation.
The vertical scale is multiplied by 2.
Fig. 11 : Photographie de la paroi sud des tranchées S14 et S15 et interprétation. L'échelle verticale a été multipliée par 2.

4.4 - STRATIGRAPHY OF THE AEOLIAN DEPOSITS

The coastal cliff stratigraphy comprises the following units from bottom to top (fig. 13):

(1) Cross-bedded sand, grey below the groundwater table (US 110), light brown above (US 109), visible over about 1 m thick. These sands correspond to a dune with an avalanche face (parabolic or barkhanoid dune). Since the lower part of the sands was saturated with water and very unstable, it was not possible to reach the top of the

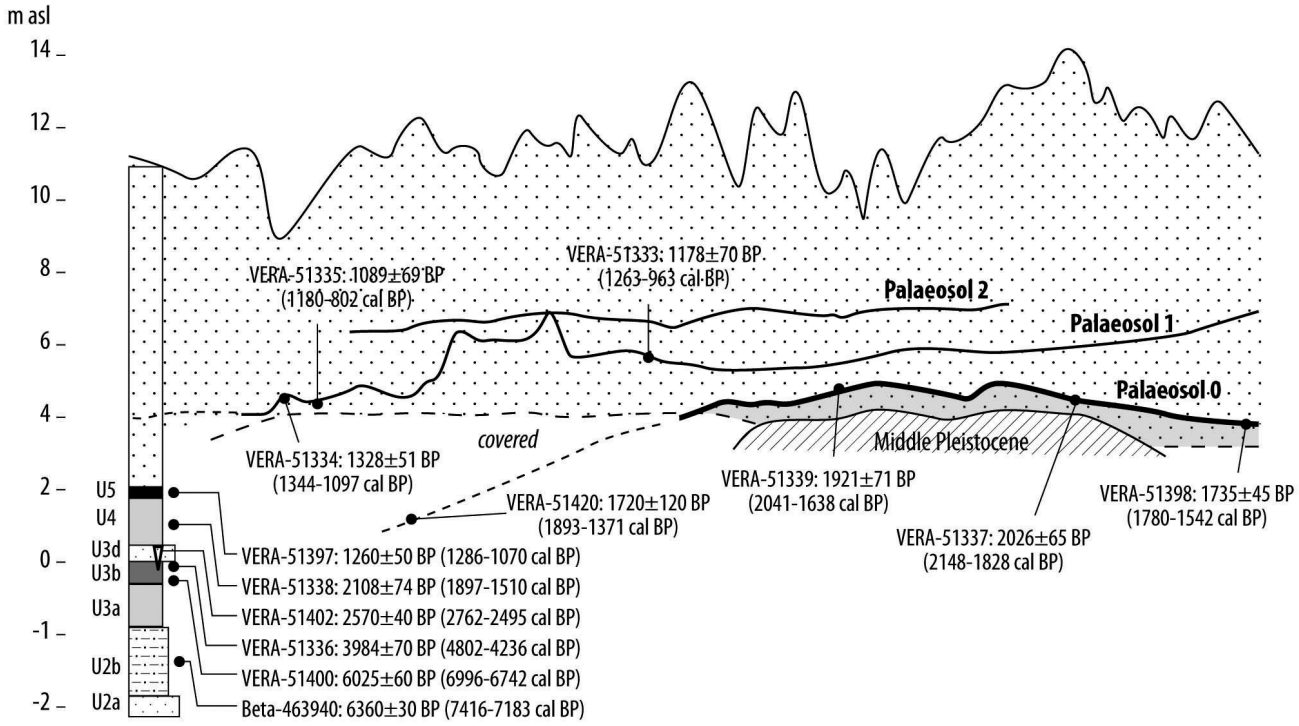

Fig. 12: Location of ^{14}C ages by Stéphan *et al* (2019), redrawn from the original publication.
Fig. 12 : Localisation des dates ^{14}C effectuées par Stéphan et al. (2019), redessiné d'après la publication.

underlying estuarine sequence. Based on the measured elevations, the peat with footprints should be about 0.5 m beneath the bottom of the trench.

(2) Massive bioturbed sand, with roots and ferruginous spots (US 108) (0.5 m thick), overlain by a 5 to 10 cm thick black humic horizon (US 107) (fig. 14D). This level corresponds to an Arenosol (P1) developed on a first dune. The elevation of the palaeosol varies significantly along the cliff, which shows that it developed at the top of a dune following a strong decrease in sand inputs and the fixation of the dune by vegetation.

(3) Light brown sands with steep cross-bedding (US 106), approximately 1.2 m thick. They indicate the emplacement of a second dune generation.

(4) Light brown sands with alternating sub-horizontal beds, beds with no visible stratification and convolute beds (US 105) (fig. 14C). The sands are light-coloured over a thickness of about 0.5 m, then become enriched in organic matter (grey-brown colour) and show abundant bioturbation (US 104) (fig. 14B, E). US 104, 0.6 to 0.8 m thick, can be considered a cumulative soil, in which the accumulation of organic matter was concomitant with substantial sandy sedimentation. This unit is an equivalent of Palaeosol 2 of Stéphan *et al.* (2019).

(5) Light brown sands with convolute bedding (US 103) similar to US 105, approximately 2 m thick.

(6) Light brown sands with subhorizontal bedding (US 102), visible over 1 m (fig. 14A) and disturbed at the top.

Additional observations were made about 200 m to the south. They show that the cross-bedded sands cover here a layer of strongly bioturbated, massive grey sand. A humic horizon already described by Stéphan *et al.* (2019) and referred to as Palaeosol 0 lies in between the two sandy units.

4.5 - CHRONOLOGICAL DATA OF THE DUNE DEPOSITS

The coastal dunefield has been the subject of IRSL dating by Clarke *et al.* (1999, 2002) in Médoc and farther south. The ages show that the emplacement of the dunes currently visible in the landscape is relatively recent. The ages are grouped into two distinct periods, the youngest between 250 and 600 BP (barkhanoid and parabolic "modern dunes") and the oldest between 1000 and 1300 BP ("primary dunes", only parabolic). Older ^{14}C ages have also been obtained from palaeosols in between sand layers at the base of the Dune du Pilat and suggest aeolian activity between 5.0 and 2.3 ka cal BP (Tastet, 1998). Similarly, Smith *et al.* (1990) found by OSL an age of 5.4 ka on bioturbed sand at the base of this dune.

In the Soulac-sur-Mer area, the only available data are those of Stéphan *et al.* (2019). Median ^{14}C ages on palaeosols range from 1985 to 1639 cal BP (35 BCE - 311 CE) for Palaeosol 0 at the base of the dune deposits, and 936 and 691 cal BP (1014 - 1259 CE) for Palaeosol 1 (equivalent to P1 in our study). These ages indicate that the two main dune generations formed between ca. 1650 and 950 cal BP (~300-1000 CE) and after 700 cal BP (after ~1250 CE).

Three samples were taken from the dune sands for OSL dating, respectively within US 109 and 106 (fig. 13, Table 2), as well as within a massive grey sand level located beneath Palaeosol 0 ca. 200 m south of the study area. The ages obtained confirm the previous estimates made from the palaeosols. The first dune generation (US 109) gave an age of 1.56 ± 0.10 ka (Shfd-19182, Early Middle Ages), while the second (US 106) gave an age of 0.49 ± 0.08 ka (Shfd-19181, Modern Period). The basal

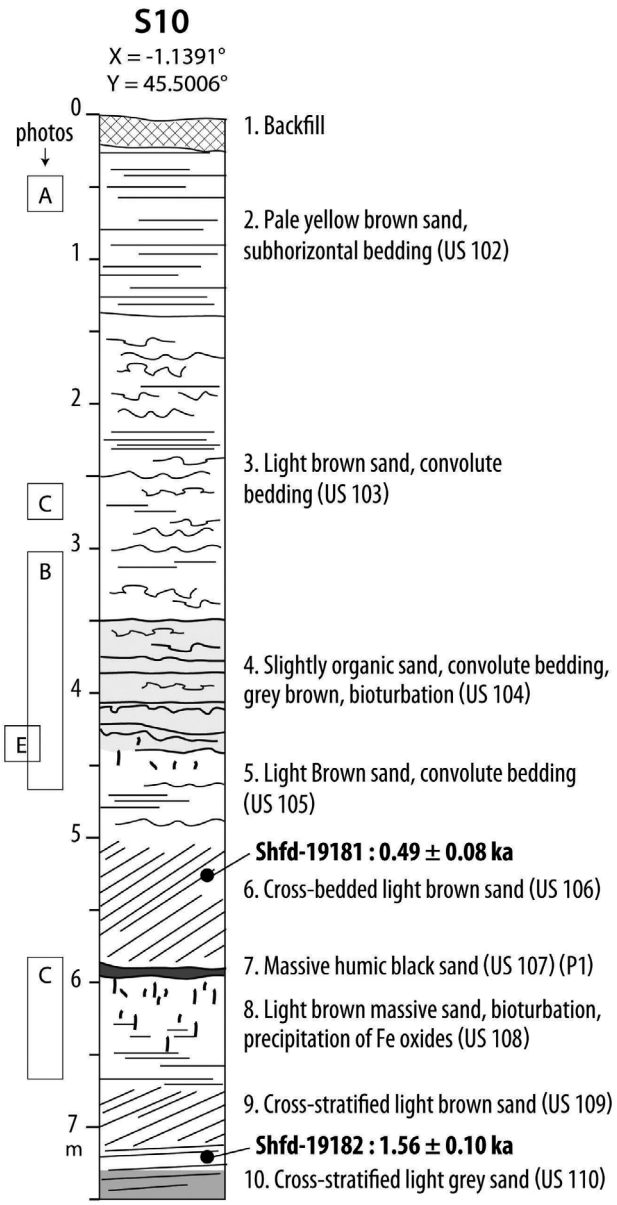

Fig. 13: Schematic section of the dunefield (S10) and location of OSL samples.
The location of the photos in Figure 14 is shown.
Fig. 13 : Coupe schématique du massif dunaire à la hauteur du sondage S10 et localisation des échantillons datés par OSL. La localisation des photos de la Figure 14 est indiquée.

massive sands collected in the south provided an age of 1.88 ± 0.14 ka (Shfd-19180), older than that of the peat with footprints (US 1002), which explains their absence in the study area.

5 - DISCUSSION

5.1 - THE ESTUARINE SEQUENCE

The sequence observed in trenches shows clays typical of a mudflat depositional context above fluvial sands (undated) and reflects the progradation of estuarine environments in a small tributary following the post-glacial sea level rise. The green clay accumulation started abruptly at -2 m to -0.8 m NGF depending on the trenches. This suggests the existence of sandy reliefs buried by the clays (onlap), whose base is, therefore, slightly diachronic. Interlayered sand-silt facies that typify estuarine deposits closer to the Gironde are lacking. The age of the beginning of clay accumulation remains loosely constrained. It ranges from around 7.1 ka cal BP (lower limit of the age of US 1021 sands) to 5.6 ka cal BP (upper limit of the age of the wood fragment collected in US 1019 clays at -0.7 m NGF).

Overall, the sections show an alternation of periods of clay sedimentation and periods when accumulation became almost null. The latter phases were associated with the development of peaty levels or partially oxidized soils with desiccation cracks, which indicate the extension of the salt marsh environments towards the estuary. These features appear especially in the upper part of the sequence, after an initial phase of homogeneous clay deposition over more than 1.5 m thick. According to available ages, this phase covers the period ranging from ca. 7.1 ka to 5.1 ka cal BP.

Sediment accretion was then more limited, probably because of the progressive filling of the marsh. Accumulation took place mainly in tidal channels, in a context richer in organic matter. The channels identified in cross-section remain poorly dated. The oldest channel predates the occupation of the Early Iron Age (~2.6 ka cal BP), probably slightly because the remains lie directly on the flood sands. The second was

ref date	sample ref.	X WGS84	Y WGS84	Z /surf. (m)	method	material	age (a)	uncertainty	lithology	references
Shfd-19180	Soulac-OSL3	-1.1438	45.4933	6.0	SAR OSL	quartz	1880	144	massive sand	Bertran et al., 2020
Shfd-19181	Soulac-OSL2	-1.1394	45.5003	5.2	SAR OSL	quartz	486	43	cross-stratified sand	Bertran et al., 2020
Shfd-19182	Soulac-OSL1	-1.1394	45.5003	7.2	SAR OSL	quartz	1563	105	cross-stratified sand	Bertran et al., 2020

Table 2: OSL ages obtained from the aeolian deposits.
Tableau 2: Ages OSL obtenus sur les dépôts éoliens.

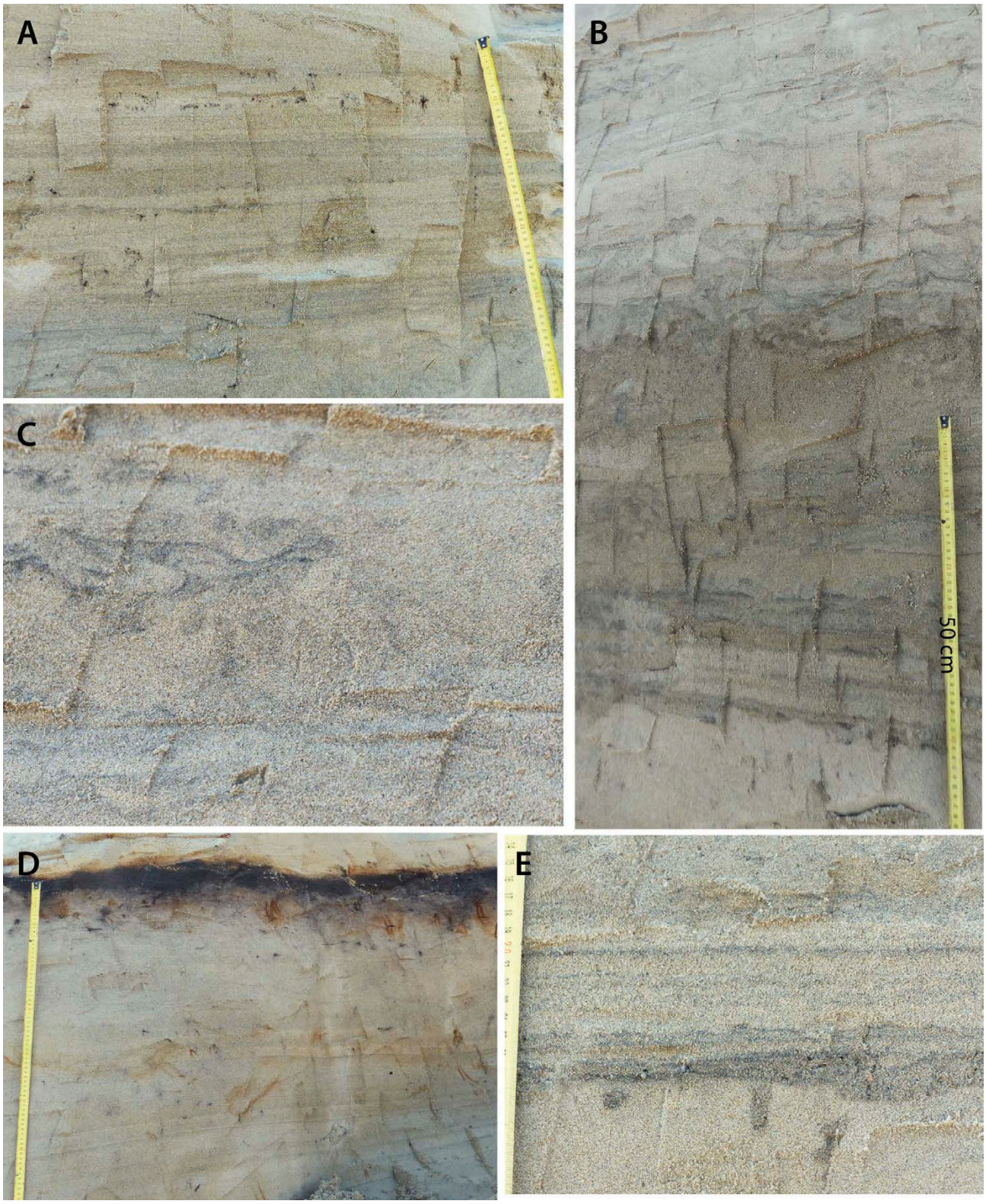

Fig. 14: Views of the facies of aeolian deposits.
A - Horizontally bedded sand, US 102; B - Slightly humic sand with convolute bedding (US 103 to 105); C - Detail of deformations; D - Palaeosol P1 (Arenosol); E - Bioturbated level (base of US 104).
Fig.14 : Vues des différents faciès des dépôts éoliens. A - Sable à litage horizontal, US 102 ; B - Sable légèrement humifère à litage convolute (US 103 à 105) ; C - Détail des déformations ; D - Paléosol P1 (Arénosol) ; E - Niveau bioturbé (base de l'US 104).

formed between the Gallo-Roman period and the Early Middle Ages. The age obtained on the middle part of the filling (~1.4 ka cal BP) is contemporary with the Early Middle Ages.

Three periods of peat development are documented in the sequence. The oldest peat yielded an age of 5.3-4.9 ka cal BP on root debris (Late Neolithic). The duration of its formation remains loosely constrained. The second level is contemporary to the Gallo-Roman occupation. The last peat with footprints dates from the end of the Early Middle Ages (1.3-1.2 ka cal BP).

Comparison of the sequence with those described

in other Gironde marshes provides new lines of understanding of the estuarine system, particularly with regard to the chronology of deposition. For this purpose, the ages obtained on the marshes of Soulac-sur-Mer (Stéphan *et al.*, 2019; this study), the Perge (Diot *et al.*, 2002), Reysson (Diot *et al.*, 1999), Talais, Monards and Saint-Ciers-sur-Gironde (Clavé, 2001) were compiled, excluding the ages obtained on archaeological material. All the marshes are located on the sides of the Gironde estuary and, therefore, are protected from the direct influence of marine morphogenesis and from the migration of depocentres typical of the estuary. The dated samples correspond to "peat", wood fragments, shells and ostracods and were calibrated according to their continental or marine origin. The samples come mainly from cores and are randomly distributed in the stratigraphy, with no identifiable sampling bias towards the most recent or, on the contrary, the oldest sedimentation phases. "Peat" (most likely organic clay with plant debris) is over-represented in the data set, which suggests a bias toward upper intertidal facies. However, Diot *et al.* (2002) showed that the dated "peat" layers in the Perge marsh are laterally in continuity with greenish grey clay located closer to the estuary and thus, potentially record a similar depositional history. Such a chronological analysis is not without pitfalls (see e.g., Chiverell *et al.*, 2011). We assume, however, that higher densities of ages roughly reflect periods with higher sediment accumulation rates. The Kernel Density Estimation (51 dates) highlights some remarkable features (fig. 15):

(1) Fine-grained sedimentation did not start before 7.7 ka cal BP in all marshes, whose basal elevation is located at -5 m NGF at most. This age/elevation pairing is in good agreement with that deduced from sea level rise according to Lambeck *et al.* (2014) and García-Artola *et al.* (2018).

(2) The estimated age distribution (KDE) broadly follows an asymmetrical curve. The probabilities increase rapidly between 7.7 and 6.5 ka cal BP to peak between 6.5 and 5.5 ka cal BP, then decrease to a low value during the last millennia. This suggests that sedimentation rates were highest between 6.5 and 5.5 ka when the marine transgression reached approximately the current sea level and the space available for sediment accumulation was the largest. This maximum is consistent with the estimated age of the first generation of estuarine clays at Soulac-sur-Mer (age between 7.1 and 4.9 ka cal BP). Sedimentation slowed after 5.5 ka cal BP, which probably reflects the reduction in the accommodation space following progressive filling of the marshes, in a context of quasi-stability of the sea level. Deceleration in sea level rise during the Mid-Holocene was likely a key factor in the development of estuarine deposits as observed worldwide (Stanley and Warnes, 1994). Additional factors such as the role of Neolithic agriculture and associated increase in sediment fluxes through rivers have been proposed by some authors (e.g., Devillers *et al.*, 2019). The relative contribution of this factor remains difficult to assess here but is considered secondary, as it cannot account for the similar evolution of estuaries in areas of the world colonized by farmers at contrasting periods.

(3) An alternation of periods marked by a drastic decrease in age probabilities and periods of high probabilities clearly appears after 5.5 ka cal BP. This pattern may in part be an artifact due to the still insufficient number of available dates. However, it is interesting to note that the majority of peaks, notably the Little Ice Age

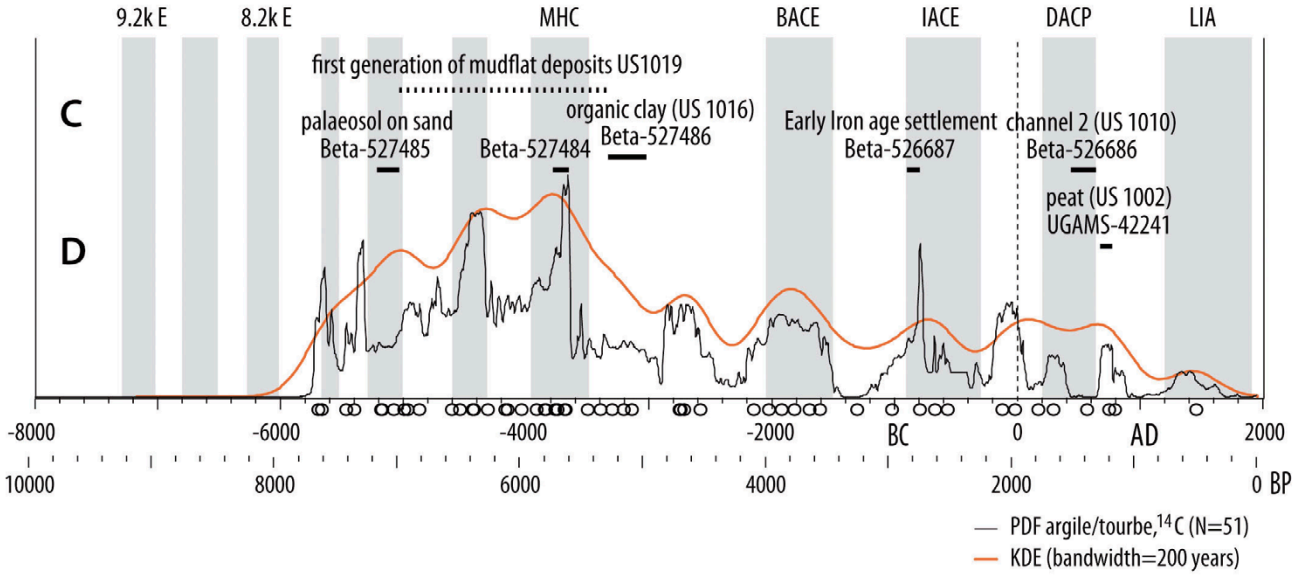

Fig. 15: Age distribution of clay and peat deposits in the Gironde estuary by Kernel Density Estimation (KDE) and Cumulated Probability Density (CPF).

The new ^{14}C ages are shown. Grey bands indicate the coldest periods, according to Kobashi *et al.* (2017). LIA: Little Ice Age, DACP: Dark Ages Cold Period, IACE: Iron Age Cold Epoch, BACE: Bronze Age Cold Epoch, MHC: Mid-Holocene Cooling, 8.2kE: 8.2 ka Event, 9.2kE: 9.2 ka Event.

Fig. 15 : Distribution des âges des dépôts estuariens argileux et tourbeux de la Gironde par estimation de densité par noyaux (KDE) et densité de probabilité cumulée (CPF). Les nouvelles dates ^{14}C sont indiquées. Les bandes grises indiquent les périodes les plus froides, d'après Kobashi et al. (2017). LIA : Petit Age Glaciaire, DACP : Dark Ages Cold Period, IACE : Iron Age Cold Epoch, BACE : Bronze Age Cold Epoch, MHC : Mid-Holocene Cooling, 8.2kE : 8.2 ka Event, 9.2kE : 9.2 ka Event.

(XIIIth-XIXth centuries CE) and the cold period of the Early Iron Age (~2.9-2.5 ka cal BP) for the most recent, correspond to well-identified periods of climate degradation (Wanner *et al.*, 2011; Kobashi *et al.*, 2017). These periods correspond to phases of increasing flood frequency in many European rivers (Macklin *et al.*, 2006; Hoffmann *et al.*, 2008). The assumption of accelerated accretion of intertidal deposits during periods of unusually high flood frequency can, therefore, be proposed. This assumption also provides an explanation for the alternation of phases of clay accumulation and phases of peat and soil development observed at Soulac-sur-Mer.

The analysis of the chronology of deposition is still preliminary and should benefit from the input of new ages. In particular, the multiplication of ages from the Soulac-sur-Mer sequence thanks to ongoing marine erosion and within a well-identified stratigraphic framework will make it possible to use the stratigraphic relationships between samples to better constrain the main sedimentation phases using Bayesian statistics.

5.2 - DUNEFIELD

In the study area, the coastal dunefield comprises two main units separated by an Arenosol (P1), which indicates a phase of sand fixation by vegetation. This palaeosol is a lateral equivalent of Palaeosol 1 described previously by Stéphan *et al.* (2019) and ^{14}C dated between 936 and 691 cal BP (~1014-1259 CE), i.e. contemporary with the Medieval Warm Period (MWP). The dune facies are not homogeneous. The basal unit OSL dated around 1.56 ka corresponds to classic avalanche-face deposits (e.g., Hunter, 1977). In the middle part (US 103 to 105), which was OSL dated around 0.49 ka, the bedding is deformed and slightly coloured by organic matter. This facies has already been described in Holocene dunes further inland by Bertran *et al.* (2011) and in other European regions (Koster *et al.*, 1993). These authors showed that syn-sedimentary bedding deformation was mainly due to trampling of the dunes by cattles, whose footprints are sometimes still identifiable on the bed surface.

The chronology of Holocene dunes in Aquitaine was recently studied in detail by Bertran *et al.* (2020) from 22 OSL dates. The analysis of the age distribution using the KDE method highlighted two main peaks of aeolian activity, one around 1.6 ka, corresponding to the Dark Ages Cold Period (DACP), the other around 0.4 ka, i.e. Little Ice Age (LIA). Several historical sources have reported on the rapid advance of coastal dunes during the LIA, particularly in Médoc where they threatened villages (Buffault, 1942). These periods of rapid dune advance have already been identified elsewhere in Europe and reflect phases of increased storm frequency (Van Vliet-Lanoë *et al.*, 2014; Jackson *et al.* 2019). In comparison, the peaks shown from the distribution of IRSL ages on feldspars published by Clarke *et al.* (1999, 2002) are shifted towards the present, probably because of methodological issues (lack of fading correction). The density peak occurring around 1.12 ka, contemporary to the Medieval Warm Period, should therefore not be retained.

6 - CONCLUSION

The archaeological works carried out on the Soulac-sur-Mer beach made it possible to clarify the sedimentary context and the stratigraphy of the estuarine and aeolian formations eroded by the ocean. The main results show that the site corresponded to a former tributary of the Gironde that was filled by estuarine and aeolian deposits during the Holocene following the sea level rise. A first phase of homogeneous estuarine mud deposition occurred between about 7.1 ka and 4.9 ka cal BP in a mudflat context. The later phases resulted in alternating phases of clay sedimentation, phases of peat and hydromorphic soil development with desiccation cracks (salt marsh), and tidal channel incision. The sequence was finally capped by peat with cattle footprints and herbaceous hummocks, presumably in a freshwater marsh context.

Comparison of the ages obtained on this sequence by Stéphan *et al.* (2019) and this study with those from other estuarine marshes bordering the Gironde shows a relatively similar evolution. The radiocarbon age distribution suggests that mud sedimentation was rapid between 6.5 and 5.5 ka cal BP throughout the marshes and then gradually slowed down owing to plugging. The alternation of sedimentation phases, peat development and soil formation phases is thought to reflect fluctuations in flood frequency during the Holocene.

The upper peat with footprints dates from the Early Middle Ages. The estuarine deposits were then buried by dune advance during the historical period. The first dune generation is contemporary with the Early Middle Ages, around 1.6 ka. This phase of rapid dune advance has also been identified elsewhere in southwest France and coincides with a climatic degradation (Dark Age Cold Period) associated with an increase in storm frequency. The second dune generation, which is strongly disturbed by cattle trampling, is dated to around 0.5 ka and is related to the Little Ice Age advance, already known through historical texts and numerical dating of the dunefield.

The continuous erosion of the coast by the Atlantic Ocean offers the opportunity to follow over large areas the stratigraphy of estuarine deposits and the various archaeological occupations. Future archaeological works should therefore contribute to renewing our understanding of human use in this specific environment.

ACKNOWLEDGEMENTS

The archaeological work was carried out by the Institut National de Recherches Archéologiques Préventives under the supervision of the Département des Recherches Archéologiques Subaquatiques (DRASM), to which we would like to express our gratitude. OSL dating was financed by the PACEA laboratory (University of Bordeaux). We would also like to thank P. Stéphan and F. Verdin for field discussions and W. O'Yl (Inrap) for the photogrammetric survey of the outcrops. B. Devillers and an anonymous reviewer are also acknowledged for their constructive remarks on the manuscript.

REFERENCES

ALLEN G.P., BOUCHET J.M., CARBONEL P. & COLLABORATORS, 1974 - Environnements et processus sédimentaires sur le littoral nord-aquitain. *Bulletin de l'Institut Géologique du Bassin d'Aquitaine,* **15**, 3-183.

BERTRAN P., BATEMAN M.D., HERNANDEZ M., MERCIER N., MILLET D., SITZIA L. & TASTET J.P., 2011 - Inland aeolian deposits of south-west France: facies, stratigraphy and chronology. *Journal of Quaternary Science,* **26**(4), 374-388.

BERTRAN P., ANDRIEUX E., BATEMAN M., FUCHS M., KLINGE M. & MAREMBERT F., 2020 - Mapping and chronology of coversands and dunes from the Aquitaine Basin, southwest France. Aeolian Research 47, 100628.

BOSQ M., BERTRAN P., BEAUVAL C., KREUTZER S., DUVAL M., BARTZ M., MERCIER N., SITZIA L. & THE LITAQ PROJECT MEMBERS, 2019 - Stratigraphy and chronology of Pleistocene coastal deposits in northern Aquitaine, France: a reinvestigation. *Quaternaire,* **30** (1), 5-20.

BUFFAULT P., 1942 - *Histoire des dunes maritimes de la Gascogne*. Imprimerie Delmas, Bordeaux, 446 p.

CLARKE M.L., RENDELL H.M. & PYE K., 1999 - Evidence for the timing of dune development on the Aquitaine Coast, southwest France. *Zeitschrift fur geomorphologie*, supplement band, **116**, 147-163.

CLARKE M., RENDELL H., TASTET J.P., CLAVE B. & MASSE L., 2002 - Late-Holocene sand invasion and North Atlantic storminess along the Aquitaine Coast, southwest France. *The Holocene*, **12** (2), 231-238.

CLAVE B., 2001 - Évolution des paléo-environnements côtiers à l'Holocène : exemple de l'Aquitaine septentrionale. PhD thesis, University of Bordeaux 1, Bordeaux, 316 p.

COURREGES M., 1997 - Le crypto-karst de la péninsule du Médoc. Crypto-altération, dissolution, karst sous-marin et évolution quaternaire. *Quaternaire,* **8** (2), 289-304.

CHIVERRELL R.C., THORNDICRAFT V.R. & HOFFMANN T.O., 2011 - Cumulative probability functions and their role in evaluating the chronology of geomorphological events during the Holocene. *Journal of Quaternary Science,* **26** (1), 76-85.

D'ALPAOS A., LANZONI S., MARANI M., BONOMETTO A., CECCONI G. & RINALDO A., 2007 - Spontaneous tidal network formation within a constructed salt marsh: Observations and morphodynamic modelling. *Geomorphology,* **91**, 186-187.

DEVILLERS, B., BONY, G., DEGEAI, J.-P., GASCO, J., LACHENAL, T., BRUNETON, H., YUNG F., OUESLATI H. & THIERRY A., 2019 - Holocene coastal environmental changes and human occupation of the lower Hérault River, southern France. *Quaternary Science Reviews,* **222**, 105912.

DIOT M.F., MARAMBAT L., MASSE L. & TASTET J.P., 1999 - Étude palynologique du remplissage holocène du Marais de Reysson, rive gauche de la Gironde, nord-Médoc (France). Relation avec l'occupation humaine. *Actes des congrès nationaux des sociétés historiques et scientifiques, Nantes, systèmes fluviaux*, 143-162.

DIOT M.F., MASSE L., COQUILLAS D. & CLAVE B., 2002 - Utilisation des groupes polliniques dans la reconstitution des paléoenvironnements holocènes du marais de la Perge - Nord Médoc - Gironde (France). Implications sur l'occupation humaine. *Revue d'Archéométrie,* **26**, 155-169.

DUBREUILH J., 1976 - *Contribution à l'étude sédimentologique du système fluviatile Dordogne-Garonne dans la région de Bordeaux*. PhD thesis, University of Bordeaux, 275 p.

DUBREUILH J. & MARIONNAUD J.M., 1972 - *Carte géologique à 1/50 000 (729-730), feuille de St-Vivien-de-Médoc et Soulac-sur-Mer*, Bureau des Recherches Géologiques et Minières, Orléans, 45 p.

ELHAÏ H. & PRENANT A., 1963 - Présence et extension d'un niveau marin littoral interglaciaire sur la côte du Médoc. *Bulletin de la société géologique de France,* **7**, 495-507.

FABRE A., 1939 - *Les terrains de revêtement du Médoc*, Bordeaux, Drouillard, 334 p.

FAYE S., EYNAUD F., BOSQ M. & COLLABORATORS, 2019 - Holocene palaeoenvironmental evolution of the Médoc peninsula (SW France): insight from the sedimentological study of the "Lède du Gurp" archaeological site. *Quaternaire,* **30** (1), 31-464.

GARCÍA-ARTOLA A., STÉPHAN P., CEARRETA A., KOPP R.E., KHAN N.S. & HORTON B.P., 2018 - Holocene sea-level database from the Atlantic coast of Europe. *Quaternary Science Reviews,* **196**, 177-192.

HOFFMANN T., LANG A. & DIKAU R., 2008 - Holocene river activity: analysing ^{14}C-dated fluvial and colluvial sediments from Germany. *Quaternary Science Reviews,* **27**, 2031-2040.

HUNTER R.E., 1977 - Basic types of stratification in small eolian dunes. *Sedimentology,* **24**, 361-387.

JACKSON D.W.T., COSTAS S. & GUISADO-PINTADO E., 2019 - Large-scale transgressive coastal dune behavior in Europe during the Little Ice Age. *Global and Planetary Change,* **175**, 82-91.

KOBASHI T., MENVIEL L., JELTSCH-THÖMMES A. & COLLABORATORS, 2017 - Volcanic influence on centennial to millennial Holocene Greenland temperature change. *Nature Scientific Reports,* **7**, 1441. DOI:10.1038/s41598-017-01451-7

KOSTER E.A., CASTEL I.I.Y. & NAP R.L., 1993 - Genesis and sedimentary structures of late Holocene aeolian drift sands in northwestern Europe. *In* K. Pye (ed.), The dynamics and environmental context of aeolian sedimentary systems. *Geological Society Special Publication,* **72**, 247-267.

LAMBECK K., ROUBY H., PURCELL A., SUN Y. & SAMBRIDGE M., 2014 - Sea level and global ice volumes from the Last Glacial Maximum to the Holocene. *PNAS* **111** (43), 15296-15303.

MACKLIN M.G, BENITO G., GREGORY K.J., JOHNSTONE E., LEWIN J., MICHCZYN´SKA D.J., SOJA R., STARKEL L. & THORNDYCRAFT V.R., 2006 - Past hydrological events reflected in the Holocene fluvial record of Europe. *Catena*, **66**, 145-154.

O'BRIEN C.E. & JONES R.L., 2003 - Early and Middle Pleistocene vegetation history of the Medoc region, southwest France. *Journal of Quaternary Science,* **18** (6), 557-579.

PONTEE N.I., TASTET J.P. & MASSE L., 1998 - Morpho-sedimentary evidence of Holocene coastal changes near the mouth of the Gironde and on the Medoc Peninsula, SW France. *Oceanologica Acta,* **21** (2), 243-261.

SITZIA L., BERTRAN P., BAHAIN J.J., BATEMAN M., HERNANDEZ M., GARON H., DE LAFONTAINE G., MERCIER N., LEROYER C., QUEFFELEC A. & VOINCHET P., 2015 - The quaternary coversands of southwest France. *Quaternary Science Reviews,* **124**, 84-105.

SMITH B.W., RHODES E.J., STOKES S., SPOONER N.A. & AITKEN M.J., 1990 - Optical dating of sediments: initial quartz results from Oxford. *Archaeometry,* **32** (1), 19-31.

STANLEY D. & WARNE A., 1994 - Worldwide initiation of Holocene marine deltas by deceleration of sea-level rise. *Science,* **265**, 228-231.

STEPHAN P., VERDIN F., ARNAUD-FASSETTA G., BERTRAND F., EYNAUD F., GARCIA-ARTOLAS A., BOSQ M., CULIOLI C., SUANEZ S., COUTELIER C., BERTRAN P., COLIN A. & COSTA S., 2019 - Holocene coastal changes along the Gironde estuary (SW France): new insights from the North Médoc Peninsula beach/dune system. *Quaternaire,* **30** (1), 47-75.

TASTET J.P., 1998 - Chronologie et cartographie d'un complexe dunaire côtier holocène, l'exemple aquitain du Nord-Médoc (France). *Quaternaire,* **9** (3), 157-167.

TASTET J.P., 1999 - Le Pléistocène de la façade atlantique du Nord-Médoc (France) : état des connaissances sur la lithologie et la chronostratigraphie des « Argiles du Gurp » s.l. *Quaternaire,* **10** (2), 199-212.

TROLARD F., 2006 - Fougerite: From field experiment to the homologation of the mineral. *C.R. Geoscience,* **338**, 1158-1166.

VAN VLIET-LANOË B., PENAUD A., HÉNAFF A., DELACOURT C., FERNANE A., GOSLIN J., HALLÉGOUËT B. & LE CORNEC E., 2014 - Middle- to late-Holocene storminess in Brittany (NW France): Part II - The chronology of events and climate forcing. *The Holocene,* **24** (4), 434-453.

VERMEESCH P., 2012 - On the visualisation of detrital age distributions. *Chemical Geology*, **312-313**, 190-194.

VIROLLE M., BRIGAUD B., BOURILLOT R., FENIES H., FORTIER E., DUTEIL T., NOUET J., PATRIER P. & BEAUFORT D., 2019 - Detrital clay grain coats in estuarine clastic deposits: origin and spatial distribution within a modern sedimentary system, the Gironde Estuary (south-west France). *Sedimentology,* **66**, 859-894.

WANNER H., SOLOMINA O., GROSJEAN M., RITZ S.P. & JETEL M., 2011 - Structure and origin of Holocene cold events. *Quaternary Science Reviews,* **30**, 3109-3123.